Atmospheric histories and emissions of chlorofluorocarbons CFC-13 ($CClF_3$), #CFC-114 ($C_2Cl_2F_4$), and CFC-115 (C_2ClF_5)

Citation: Vollmer, Martin K., Dickon Young, Cathy M. Trudinger, Jens Mühle, Stephan Henne, Matthew Rigby, Sunyoung Park, et al. "Atmospheric histories and emissions of chlorofluorocarbons CFC-13 ($CClF_3$), ΣCFC-114 ($C_2Cl_2F_4$), and CFC-115 (C_2ClF_5)." Atmospheric Chemistry and Physics 18, 2 (January 2018): 979–1002 © 2018 The Authors

As Published: http://dx.doi.org/10.5194/acp-18-979-2018

Publisher: Copernicus Publications

Persistent URL: http://hdl.handle.net/1721.1/113703

Version: Final published version: final published article, as it appeared in a journal, conference proceedings, or other formally published context

Atmos. Chem. Phys., 18, 979–1002, 2018
https://doi.org/10.5194/acp-18-979-2018

Atmospheric Chemistry and Physics
Open Access
EGU

Atmospheric histories and emissions of chlorofluorocarbons CFC-13 ($CClF_3$), ΣCFC-114 ($C_2Cl_2F_4$), and CFC-115 (C_2ClF_5)

Martin K. Vollmer[1], Dickon Young[2], Cathy M. Trudinger[3], Jens Mühle[4], Stephan Henne[1], Matthew Rigby[2], Sunyoung Park[5], Shanlan Li[5], Myriam Guillevic[6], Blagoj Mitrevski[3], Christina M. Harth[4], Benjamin R. Miller[7,8], Stefan Reimann[1], Bo Yao[9], L. Paul Steele[3], Simon A. Wyss[1], Chris R. Lunder[10], Jgor Arduini[11,12], Archie McCulloch[2], Songhao Wu[5], Tae Siek Rhee[13], Ray H. J. Wang[14], Peter K. Salameh[4], Ove Hermansen[10], Matthias Hill[1], Ray L. Langenfelds[3], Diane Ivy[15], Simon O'Doherty[2], Paul B. Krummel[3], Michela Maione[11,12], David M. Etheridge[3], Lingxi Zhou[16], Paul J. Fraser[3], Ronald G. Prinn[15], Ray F. Weiss[4], and Peter G. Simmonds[2]

[1]Laboratory for Air Pollution and Environmental Technology, Empa, Swiss Federal Laboratories for Materials Science and Technology, Überlandstrasse 129, 8600 Dübendorf, Switzerland
[2]Atmospheric Chemistry Research Group, School of Chemistry, University of Bristol, Bristol, UK
[3]Climate Science Centre, CSIRO Oceans and Atmosphere, Aspendale, Victoria, Australia
[4]Scripps Institution of Oceanography, University of California at San Diego, La Jolla, California, USA
[5]Kyungpook Institute of Oceanography, Kyungpook National University, South Korea
[6]METAS, Federal Institute of Metrology, Lindenweg 50, Bern-Wabern, Switzerland
[7]Earth System Research Laboratory, NOAA, Boulder, Colorado, USA
[8]Cooperative Institute for Research in Environmental Sciences, University of Colorado, Boulder, Colorado, USA
[9]Meteorological Observation Centre (MOC), China Meteorological Administration (CMA), Beijing, China
[10]Norwegian Institute for Air Research, Kjeller, Norway
[11]Department of Pure and Applied Sciences, University of Urbino, Urbino, Italy
[12]Institute of Atmospheric Sciences and Climate, Italian National Research Council, Bologna, Italy
[13]Korea Polar Research Institute, KIOST, Incheon, South Korea
[14]School of Earth and Atmospheric Sciences, Georgia Institute of Technology, Atlanta, Georgia, USA
[15]Center for Global Change Science, Massachusetts Institute of Technology, Cambridge, Massachusetts, USA
[16]Chinese Academy of Meteorological Sciences (CAMS), China Meteorological Administration (CMA), Beijing, China

Correspondence: Martin K. Vollmer (martin.vollmer@empa.ch)

Received: 8 October 2017 – Discussion started: 10 October 2017
Revised: 6 December 2017 – Accepted: 11 December 2017 – Published: 25 January 2018

Abstract. Based on observations of the chlorofluorocarbons CFC-13 (chlorotrifluoromethane), ΣCFC-114 (combined measurement of both isomers of dichlorotetrafluoroethane), and CFC-115 (chloropentafluoroethane) in atmospheric and firn samples, we reconstruct records of their tropospheric histories spanning nearly 8 decades. These compounds were measured in polar firn air samples, in ambient air archived in canisters, and in situ at the AGAGE (Advanced Global Atmospheric Gases Experiment) network and affiliated sites. Global emissions to the atmosphere are derived from these observations using an inversion based on a 12-box atmospheric transport model. For CFC-13, we provide the first comprehensive global analysis. This compound increased monotonically from its first appearance in the atmosphere in the late 1950s to a mean global abundance of 3.18 ppt (dry-air mole fraction in parts per trillion, pmol mol^{-1}) in 2016. Its growth rate has decreased since the mid-1980s but has remained at a surprisingly high mean level of 0.02 ppt yr^{-1} since 2000, resulting in a continuing growth of CFC-13 in the atmosphere. ΣCFC-114 increased from its appearance in the 1950s to a maximum of 16.6 ppt in the early 2000s and has since slightly declined to 16.3 ppt in 2016. CFC-115 increased monotonically from its first appearance in the 1960s and reached a global mean mole frac-

tion of 8.49 ppt in 2016. Growth rates of all three compounds over the past years are significantly larger than would be expected from zero emissions. Under the assumption of unchanging lifetimes and atmospheric transport patterns, we derive global emissions from our measurements, which have remained unexpectedly high in recent years: mean yearly emissions for the last decade (2007–2016) of CFC-13 are at $0.48 \pm 0.15\,\mathrm{kt\,yr^{-1}}$ ($> 15\,\%$ of past peak emissions), of ΣCFC-114 at $1.90 \pm 0.84\,\mathrm{kt\,yr^{-1}}$ ($\sim 10\,\%$ of peak emissions), and of CFC-115 at $0.80 \pm 0.50\,\mathrm{kt\,yr^{-1}}$ ($> 5\,\%$ of peak emissions). Mean yearly emissions of CFC-115 for 2015–2016 are $1.14 \pm 0.50\,\mathrm{kt\,yr^{-1}}$ and have doubled compared to the 2007–2010 minimum. We find CFC-13 emissions from aluminum smelters but if extrapolated to global emissions, they cannot account for the lingering global emissions determined from the atmospheric observations. We find impurities of CFC-115 in the refrigerant HFC-125 (CHF_2CF_3) but if extrapolated to global emissions, they can neither account for the lingering global CFC-115 emissions determined from the atmospheric observations nor for their recent increases. We also conduct regional inversions for the years 2012–2016 for the northeastern Asian area using observations from the Korean AGAGE site at Gosan and find significant emissions for ΣCFC-114 and CFC-115, suggesting that a large fraction of their global emissions currently occur in northeastern Asia and more specifically on the Chinese mainland.

1 Introduction

Chlorofluorocarbons (CFCs) are very stable man-made compounds known to destroy stratospheric ozone. For this reason they were regulated for phase-out under the Montreal Protocol on Substances that Deplete the Ozone Layer and its subsequent amendments. The ban has been effective since the end of 1995 for developed countries and the end of 2010 for developing countries. The ban is put on production for emissive use and does not cover production for feedstock or recycling of used CFCs for recharging of old equipment, the latter being applied particularly in the refrigeration sector. While the dominant CFCs in the atmosphere are CFC-12 (CCl_2F_2), CFC-11 (CCl_3F), and CFC-113 ($C_2Cl_3F_3$), this article reports on CFC-13 (chlorotrifluoromethane, $CClF_3$), ΣCFC-114, here defined as the combined isomer 1,2-dichlorotetrafluoroethane ($CClF_2CClF_2$, CFC-114, CAS 76-14-2) and 1,1-dichlorotetrafluoroethane (CCl_2FCF_3, CFC-114a, CAS 374-07-2), and CFC-115 (chloropentafluoroethane, C_2ClF_5). The compounds were mainly used in specialized refrigeration; hence, their abundances in the atmosphere are considerably smaller than those of the three major CFCs. However, their atmospheric lifetimes are significantly longer (see Table 1 for climate metrics). Ozone depletion potentials (ODPs) for the three compounds are high and their radiative efficiencies are high, thereby yielding high global warming potentials (GWPs), with those for CFC-13 (13 900 for GWP-100 yr and $\sim$ 16 000 for GWP-500 yr) only surpassed by very few other greenhouse gases.

Removal of these CFCs from the atmosphere occurs predominantly in the stratosphere through ultraviolet (UV) photolysis and reaction with excited atomic oxygen ($O(^1D)$), and to a lesser extent by Lyman-α photolysis in the mesosphere. The atmospheric lifetime for CFC-13 of 640 years used in the present study is based on a study by Ravishankara et al. (1993) and is dominated (80 %) by the removal through reaction with $O(^1D)$; see Table 1. The lifetimes for CFC-114 and CFC-115 have recently been revised as part of the SPARC (Stratosphere–troposphere Processes And their Role in Climate) lifetimes assessment (SPARC, 2013). In that study the lifetime of CFC-114 was reported as 189 years (153–247 years) with 72 % of the loss from UV photolysis and 28 % from reaction with $O(^1D)$ (Burkholder and Mellouki, 2013). However, our closer inspection of the literature from laboratory studies, used to derive UV absorption spectra and $O(^1D)$ reaction rates (Sander et al., 2011), suggests that no consideration was given in these older studies with regard to potential impurities of CFC-114a in CFC-114. Such impurities are likely present (Supplement, Laube et al., 2016), in which case they could have biased the CFC-114 UV absorption spectra, leading to an underestimate of its lifetime, as its absorption is significantly weaker compared to that of CFC-114a in the critical photolysis wavelength region (Davis et al., 2016; J. B. Burkholder, personal communication, November 2017). $O(^1D)$ kinetics for the two isomers are similar and hence would not have affected lifetime estimates as much if such impurities were present (Baasandorj et al., 2011, 2013; Davis et al., 2016). For CFC-115 the lifetime has been significantly reduced from 1700 years in earlier studies (Ravishankara et al., 1993) to 540 years (404–813 years) (SPARC, 2013) mainly due to significantly revised $O(^1D)$ kinetics (Baasandorj et al., 2013). This revised lifetime gives 37 % of the loss derived from UV photolysis and 63 % from reaction with $O(^1D)$ and a minor contribution from Lyman-α photolysis (Burkholder and Mellouki, 2013).

CFC-13 and its R-503 blend with 40 % by mass of HFC-23 (CHF_3) have been used as special-application low-temperature refrigerants (IPCC/TEAP, 2005; Calm and Hourahan, 2011) but small enhancements in CFC-13 were also found in the emissions from aluminum plants (Harnisch, 1997; Penkett et al., 1981). CFC-13 could also be present as an impurity in CFC-12 (CCl_2F_2) due to over-fluorination during production.

Reports on atmospheric CFC-13 in peer-reviewed articles are rare. Early measurements were reported on by Rasmussen and Khalil (1980), Penkett et al. (1981), and Fabian et al. (1981), who measured a first atmospheric vertical profile of this compound. CFC-13 measurements were made by Oram (1999) in the samples of the Southern Hemisphere Cape Grim Air Archive (CGAA) covering 1978–1995. He found increasing mole fractions from 1.2 pptv (therein re-

Table 1. Evolution of atmospheric metrics of CFC-13 ($CClF_3$), CFC-114 ($CClF_2CClF_2$), CFC-114a (CCl_2FCF_3), and CFC-115 (C_2ClF_5).

	CFC-13	CFC-114[a]	CFC-114a	CFC-115
Ozone depletion potential (ODP)				
in Montreal Protocol[b]	1.0	1.0	–	0.6
semiempirical, WMO 2010[c]	–	0.58	–	0.57
semiempirical, WMO 2014[d]	–	0.50	–	0.26
ODP uncertainties, Velders and Daniel (2014)[e]	–	37/30 %	–	34/32 %
Global warming potential (GWP): 100 years (500 years)				
WMO 2010[c]	14 400 (16 400)	9180 (6330)	–	7230 (9120)
IPCC 2013[f]	13 900	8590	–	7670
WMO 2014[g]	13 900	8590	–	7670
Velders and Daniel (2014) [h]	–	9170 (28 %) (6310 (36 %))	–	6930 (27 %) (7520 (34 %))
Totterdill et al. (2016)	–	–	–	8060
Davis et al. (2016)	–	–	6510	–
Atmospheric lifetime (year)				
Ravishankara et al. (1993) [i]	640	300	–	1700
WMO 2006[j]	640	300	–	1700
WMO 2010[k]	640	190	–	1020
Baasandorj et al. (2013)	–	214 (210–217)	–	574 (528–625)
SPARC (2013)[l]	–	189 (153–247)	–	540 (404–813)
WMO 2014[m]	640	189 (153–247)	–	540 (404–813)
Totterdill et al. (2016)	–	–	–	492 ± 22
Davis et al. (2016) [n]	–	–	105 (103–107)	–
Laube et al. (2016) [o]	–	–	102 (82–133)	–

[a] Literature suggests that CFC-114 climate metrics were derived from laboratory studies for the CFC-114 ($CClF_2CClF_2$) isomer alone (Sander et al., 2011, and references therein). However, in these studies there is no indication of removal of potential CFC-114a (CCl_2FCF_3) impurities, which could have caused biases in the results, e.g., leading to an underestimate of the CFC-114 lifetime due to larger UV photolysis rates for the CFC-114a (lifetime of 105 years; Davis et al., 2016).
[b] Handbook for the Montreal Protocol (UNEP, 2017).
[c] WMO Scientific Assessment of Ozone Depletion 2010 (Daniel and Velders, 2011).
[d] WMO Scientific Assessment of Ozone Depletion 2014 (Harris and Wuebbles, 2014) using the lifetimes from SPARC (2013) and the fractional release values from Montzka and Reimann (2011).
[e] Absolute values as in WMO Scientific Assessment of Ozone Depletion 2014. Uncertainties are ± for "possible"/"most likely" (on a 95 % confidence interval).
[f] IPCC (Intergovernmental Panel on Climate Change) 2013 (Myhre et al., 2013) based on Hodnebrog et al. (2013).
[g] WMO Scientific Assessment of Ozone Depletion 2014 (Harris and Wuebbles, 2014).
[h] Updates of WMO Scientific Assessment of Ozone Depletion 2010 with lifetimes from SPARC (2013) and "possible" uncertainty ranges (±, 95 % confidence interval).
[i] Ravishankara et al. (1993) give a lower limit value of 380 years for CFC-13 based on the assumption of a faster vertical mesospheric mixing.
[j] WMO Scientific Assessment of Ozone Depletion 2006 (Clerbaux and Cunnold, 2007).
[k] WMO Scientific Assessment of Ozone Depletion 2010 (Montzka and Reimann, 2011).
[l] Stratosphere–troposphere Processes And their Role in Climate (SPARC); SPARC (2013).
[m] WMO Scientific Assessment of Ozone Depletion 2014 (Carpenter and Reimann, 2014).
[n] Ranges in parentheses are due to the 2σ uncertainty in the UV absorption spectra and $O(^1D)$ rate coefficients included in the model calculations.
[o] Laube et al. (2016) adopted an uncertainty range of 83–133 years analogous with the range for CFC-114 from SPARC (2013).

ported in parts per trillion by volume) in 1978 to 3.5 pptv in 1995. Emissions deduced for this period peaked in 1987 at 3.6 kt yr^{-1}. Culbertson et al. (2004) published long records of CFC-13 measurements in background air from stations in the USA and Antarctica. For their longest record from Cape Meares (Oregon, USA), they reported a near-constant growth of CFC-13 for the earlier part of the record, with the tropospheric abundance leveling off in the late 1990s at $\sim$ 3.5 pptv.

ΣCFC-114 was used as refrigerant, blowing agent, and aerosol propellant (Fisher and Midgley, 1993; IPCC/TEAP, 2005). ΣCFC-114 is listed as a refrigerant in blends R-400 with CFC-12 in various proportions, and in R-506 with 55 % by mass HCFC-31 (CH_2ClF) (IPCC/TEAP, 2005; Calm and Hourahan, 2011). It was also used unblended in specialized refrigeration, e.g., in US naval equipment from which it was phased out over the course of several decades following the Montreal Protocol ban (Toms et al., 2004; IPCC/TEAP, 2005). Uranium isotope effusion is a process that, at least in the past, involved significant amounts of ΣCFC-114 for cooling, but now perfluorocarbons are used as a substitute (IPCC/TEAP, 2005).

Some of the first ΣCFC-114 measurements were conducted at urban sites in the 1970s by Singh et al. (1977), who reported an elevated mole fraction of up to 170 ppt (parts per trillion or pmol mol^{-1}). Measurements in background air followed (Singh et al., 1979) and a transect across the Equator in 1981 showed a global mole fraction of 14 ppt (Singh et al., 1983). In the early 1980s Fabian et al. (1981, 1985) measured vertical profiles of ΣCFC-114 in the atmosphere and found a decreasing mole fraction from 10.5 pptv at 10 km to 2.7 pptv at 35 km. Hov et al. (1984) measured ΣCFC-114 of 10.9 ppt in samples collected from Spitsbergen in spring 1983 and Schauffler et al. (1993) reported on measurements of ΣCFC-114 near the tropical tropopause. Chen et al. (1994) measured vertical profiles and a first multiyear record in both hemispheres, showing increases in CFC-114 at Hokkaido from 10 pptv in 1986 to 15 pptv in 1993 and a first indication of a slow-down of the atmospheric growth. This was also the first group that separated CFC-114 from CFC-114a. Oram (1999) also separated the two isomers and measured records from the CGAA covering 1978–1995 showing increases from 8.5 to 16.5 pptv for CFC-114 and from 0.55 to 1.75 pptv for CFC-114a. These results showed, for the first time, an increasing ratio of CFC-114a / CFC-114 in the atmosphere

and, given a shorter lifetime of CFC-114a compared to CFC-114, pointed to an increasing CFC-114a / CFC-114 emission ratio over time. The first high-frequency measurements of ΣCFC-114 from Cape Grim for 1998 and 1999 showed an abundance of 16.7 ppt, no pollution events in the footprint of the station, and no detectable trend (Sturrock et al., 2001). A first atmospheric long-term record of ΣCFC-114 was published by Sturrock et al. (2002) based on firn air measurements from Antarctica and using the CGAA record from Oram (1999), revealing an onset of growth of this compound in the atmosphere in the early 1960s. Martinerie et al. (2009) modeled atmospheric ΣCFC-114 records based on several firn air profiles and found a much earlier atmospheric appearance and larger abundances until approximately 1980 compared to Sturrock et al. (2002). In a recent study, Laube et al. (2016) reconstructed atmospheric CFC-114 and CFC-114a histories of abundances and emissions based on CGAA and firn air measurements. The study confirmed the temporally variable ratio of the two isomer abundances, and revealed a CFC-114a / CFC-114 emission ratio that increased sharply in the early 1990s but gradually declined thereafter.

CFC-115 was used as refrigerant R-115 and also occurred in blends R-502 with 49 % by mass HCFC-22 ($CHClF_2$) and R-504 with 48 % by mass HFC-32 (CH_2F_2) (Calm and Hourahan, 2011; IPCC/TEAP, 2005; Fisher and Midgley, 1993). It has also been used as an aerosol propellant and to a minor extent as a dielectric fluid (Fisher and Midgley, 1993). The first measurements of CFC-115 were made by Penkett et al. (1981) and Fabian et al. (1981), who reported on an atmospheric vertical profile. These were later complemented by more vertical atmospheric profiles (Pollock et al., 1992; Schauffler et al., 1993; Fabian et al., 1996). Later temporal records of ground-based measurements based on flask samples were published by Oram (1999) for the CGAA and Culbertson et al. (2004) for both hemispheres. Sturrock et al. (2001) reported on the first in situ measurements of CFC-115 at ~ 8 ppt for Cape Grim for 1998/99 with a small growth of $\sim 5\,\%\,\mathrm{yr}^{-1}$. The abovementioned firn air analysis by Sturrock et al. (2002) produced a first long-term record of CFC-115 and showed significantly higher abundances for the 1980s compared with the CGAA record measured by Oram (1999). In contrast, CFC-115 reconstruction by Martinerie et al. (2009) was much in agreement with the early results from the CGAA record (Oram, 1999).

Here we report on measurements of CFC-13, ΣCFC-114, and CFC-115 from the Advanced Global Atmospheric Gases Experiment (AGAGE) and affiliated networks and from measurements in archived air samples of the CGAA and the Northern Hemisphere. We further report on measurements from air samples collected from polar firn in both hemispheres, which we interpret using a firn air model. For each of the three compounds, all measurements are made and reported against a single primary calibration scale. Our observations are used with the AGAGE 12-box model and two inversion systems to derive global emissions. We further apply an inversion system to estimate regional emissions of CFC-115 from northeastern Asia for the years 2012–2016. For CFC-13, this is the first comprehensive study available on atmospheric abundances and emissions.

2 Methods

2.1 Stations and data records for in situ and flask measurements

The present study includes in situ measurements at the stations of the AGAGE (https://agage.mit.edu/) and its affiliated networks (Fig. 1). Measurements reported here are mostly based on Medusa gas chromatography mass spectrometry (GCMS) techniques (Miller et al., 2008). In Europe, measurements are made at Zeppelin (Ny Ålesund, Spitsbergen), Mace Head (Ireland), Jungfraujoch (Switzerland), and Monte Cimone (Italy), the latter being equipped with different instrumentation (Maione et al., 2013). Measurements are further conducted at Trinidad Head (California, USA), Ragged Point (Barbados), Cape Matatula (American Samoa), and Cape Grim (Tasmania, Australia). The East Asian region is covered by stations at Gosan (Jeju Island, South Korea) and Shangdianzi (China). In addition to these in situ measurements, we also include measurements of samples collected weekly since 2007 at the South Korean Antarctic station King Sejong, King George Island (South Shetland Islands) and analyzed at the Swiss Federal Laboratories for Materials Science and Technology (Empa) using Medusa GCMS technologies (Vollmer et al., 2011). We also provide a qualitative description of measurements in urban areas from Tacolneston (Great Britain, 100 km northeast of London), Dübendorf (outskirts of Zurich, Switzerland), La Jolla (outskirts of San Diego, USA), and Aspendale (outskirts of Melbourne, Australia). At a few AGAGE stations, measurements of ΣCFC-114 and CFC-115 were previously made with different GCMS instrumentation (adsorption–desorption system; Simmonds et al., 1995); however, the precisions and standard propagations of these early measurements are significantly poorer than those using Medusa GCMS technology and hence these results are not included in the present analysis.

Most of the AGAGE network observations for the three CFCs are published here for the first time in a journal article. However, some of the measurements have been previously used in the Scientific Assessment of Ozone Depletion (e.g., Carpenter and Reimann, 2014), in modeling studies to derive global emissions (Rigby et al., 2014), and for Cape Grim were reported in the journal Baseline series starting with the 1997–1998 issue. The in situ data are available directly from the AGAGE website (https://agage.mit.edu/) and data reposiories mentioned therein.

Figure 1. Sampling locations for the chlorofluorocarbons CFC-13, ΣCFC-114, and CFC-115 used in this analysis. Filled red diamonds are field sites of AGAGE (Advanced Global Atmospheric Gases Experiment) and related networks, green filled squares are urban sites, the cyan triangles denote the sampling stations for the firn air samples, and the yellow filled circle is for the flask sampling site King Sejong, Antarctica.

2.2 Archived air

Our analysis includes the results from Medusa GCMS measurements of CGAA samples collected for archival purposes since 1978 at the Cape Grim Baseline Air Pollution Station (Fig. 1). The CGAA includes > 100 samples mostly collected in 34 L internally electropolished stainless steel canisters using cryogenic sampling techniques (Fraser et al., 1991; Langenfelds et al., 1996, 2014; Fraser et al., 2016). Most samples were analyzed on the Medusa 9 instrument in 2006 at CSIRO (Aspendale, Australia) using Medusa GCMS technology with a Medusa-standard PoraBOND Q chromatography column (Miller et al., 2008). In 2011 many samples were reanalyzed and newly added samples were analyzed for CFC-13 and ΣCFC-114 on the same instrument but fitted with a GasPro chromatography column (Ivy et al., 2012). In 2016 all three compounds discussed here were reanalyzed and newly added samples were analyzed on the same instrument fitted with a GasPro column and an additional GasPro pre-column (Vollmer et al., 2016). All samples collected since 2004 are also analyzed on the Cape Grim-based Medusa-3 instrument. A comparison of the different analysis sets is provided in the Supplement and shows good agreement, indicating stability of the three CFCs in the internally electropolished canisters. For the present analysis we use the mean of the measured mole fractions from these three analysis sets.

Archived air samples from the Northern Hemisphere (NH) are also included in this study. These > 100 samples were collected at various sites and cover the period from 1973 to 2016. The majority of the samples were provided by the Scripps Institution of Oceanography (SIO) and collected at La Jolla and at Trinidad Head (California, USA). All samples were analyzed at SIO on a Medusa-1 instrument. These NH archive air samples were not exclusively collected for archival purposes and potentially include some collected during non-background conditions (influenced by emission sources) or with nonconservative sampling techniques. Consequently, rigorous data processing was necessary to limit the record to results deemed representative of broad atmospheric regions far from emission sources (hereafter termed "background"). In particular, the earlier record of ΣCFC-114 proved not useful for the present analysis because there were too many anomalous sample measurement results. Numerical results for the NH and the CGAA measurements are given in the Supplement.

2.3 Air entrapped in firn

Our data sets are complemented by measurements of the three CFCs in air entrapped in firn from samples collected in Antarctica and Greenland (Fig. 1). The Antarctic samples were collected in 1997–1998 at the DSSW20K site (66.77° S, 112.35° E, 1200 m a.s.l., ∼ 20 km west of the deep DSS drill site near the summit of Law Dome, East Antarctica; Trudinger et al., 2002; Sturrock et al., 2002), and one deep sample originates from the South Pole in 2001 (Butler et al., 2001). The Greenland firn air samples used in the present analysis were collected near the northwestern Greenland ice drill site NEEM (North Greenland Eemian Ice Drilling) at 77.45° N, 51.06° W, 2484 m a.s.l. in 2008 (NEEM-2008, EU hole, Buizert et al., 2012). Due to the remote locations of these sites, these samples are considered as representative of background air. More details on these samples and on their analysis are described by Vollmer et al. (2016) and Trudinger et al. (2016). Results for ΣCFC-114 and CFC-115 from the

DSSW20K firn air profile based on older measurement technologies and interpreted with an old version of the CSIRO firn diffusion model were previously reported by Sturrock et al. (2002) and are compared to our measurements in the Supplement.

2.4 Measurement techniques and instrument calibration

Almost all measurements reported here are conducted with Medusa GCMS instruments (Miller et al., 2008). Typically a sample is pre-concentrated on a first cold trap filled with HayeSep D and held at $\sim -160\,^{\circ}\mathrm{C}$ before it is cryo-focused onto a second trap at similar temperature, and in this process, remnants of oxygen and nitrogen and significant fractions of carbon dioxide and some noble gases are removed. The sample is then injected onto the chromatographic column (CP-PoraBOND Q, 0.32 mm ID × 25 m, 5 µm, Varian Chrompack, batch-made for AGAGE applications) of the GC instrument (Agilent 6890), purged with helium (grade 6.0), which is further purified using a getter (HP2, VICI, USA). The sample is then detected in the quadrupole mass spectrometer in selected ion mode (initially Agilent model 5973 with upgrades to model 5975 over time for most stations).

In the Medusa GCMS technology, separation of CFC-114 from CFC-114a is not possible; hence, the measurements include the cumulative abundances of the two isomers (ΣCFC-114). This leads to a potential bias compared to the numeric sum of the separated, individually measured isomers due to potentially differing molar sensitivities of the mass spectrometer for the two isomers and the fact that the ratios of the two isomers in the measured samples are likely to differ from those in the reference material used to propagate the primary calibration scales (Laube et al., 2016). We estimate a maximum potential bias of $< 2\,\%$ for our measurements (see Supplement).

For each of the three CFCs at least two fragments are routinely measured. While a target ion is used for the quantification of the peak size, the qualifying ions are mainly used for quality control by assessing the peak size ratio to the target ion, most importantly to check for potential co-elution with compounds that share the target ion. CFC-13 is measured with the target ion $C^{35}ClF_2^+$ (with a mass / charge, m/z, 85) and the qualifying ions CF_3^+ (m/z 69) and $C^{37}ClF_2^+$ (m/z 87). On the PoraBOND Q column this compound elutes near HFC-32 (CH_2F_2) and precedes ethane by ~ 2 s. ΣCFC-114 is measured with the target ion $CF_2C^{35}ClF_2^+$ (m/z 135) and the qualifying ions $CF_2C^{37}ClF_2^+$ (m/z 137) and $C^{35}ClF_2^+$ (m/z 85). It elutes a few seconds after H-1211 ($CBrClF_2$) and co-elutes with n-butane. CFC-115 is measured with the target ion $CF_2CF_3^+$ (m/z 119) and the qualifying ions $CF_2C^{35}ClF_2^+$ (m/z 135) and $CF_2C^{37}ClF_2^+$ (m/z 137). It elutes ~ 12 s after HFC-125 (CHF_2CF_3) and ~ 15 s before HFC-134a (CH_2FCF_3). Some of the instruments are set to only acquire two fragments instead of three and for some the sequences of target and qualifying ions are different from the abovementioned orders.

ΣCFC-114 measurements in strongly polluted air samples at some stations (mainly urban) have shown an analytic interference, which is believed to suppress the MS response to the quantities present in the sample. Although not fully understood, the interference is suspected to derive from large amounts of n-butane, which co-elutes with ΣCFC-114. A decrease in ΣCFC-114 of 0.20 ppt is estimated for an increase in n-butane of 1.0 ppb (parts per billion, $\mathrm{nmol\,mol^{-1}}$). The measurements of ΣCFC-114 used in the present analysis derive from air samples not significantly polluted with n-butane where the suppression effect is estimated to be smaller than the precision of the measurement. More information is provided in the Supplement.

The sample preparation and analysis time is 60–65 min. For the in situ measurements, samples are directed onto the first trap by means of a small membrane pump from a continuously flushed sampling line. In general, each air sample measurement is bracketed by measurements of a quaternary working standard that allows tracking and correction of the MS sensitivity change. The quaternary standards are whole-air samples compressed to 65 bar in 34 L internally electropolished stainless steel canisters (Essex Industries, Missouri, USA). These are collected by the individual groups within AGAGE at various sites during relatively clean air conditions using modified oil-less diving compressors (Rix Industries, USA) or cryogenic techniques. The repeated quaternary standard measurements are used to determine the measurement precisions. For CFC-13 they are $\sim 1.5\,\%$ (1σ) for the Agilent 5973 MSs and $\sim 1\,\%$ for the newer Agilent 5975 MSs. For ΣCFC-114 the precisions range from 0.2 to 0.3 % and for CFC-115 from 0.4 to 0.8 %, also showing some improvements with the change to the Agilent 5975 MSs.

As part of the network's calibration scheme and to assess for potential drift of the compounds in the canisters, the quaternary standards are compared once a week on-site with tertiary standards. These are provided by the central calibration facility at SIO and are also whole-air standards in Essex Industries canisters filled under clean air conditions at Trinidad Head or La Jolla (California, USA). These tertiary standards are measured at SIO against secondary whole-air standards before they are shipped to the sites and again after their return at the end of their usage times. They are also measured on-site against the previous and next tertiaries. The secondary standards and the synthetic primary standards at SIO provide the core of the AGAGE calibration scheme (Prinn et al., 2000; Miller et al., 2008).

2.5 Calibration scales

AGAGE has been measuring CFC-13 for many years but so far none of these data have been published. This was, among other reasons, due to the use of an interim calibration scale, which was not well defined as it was based on a dilution of

a commercial reference gas. The present study prompted the creation of a primary calibration scale for CFC-13 in the parts per trillion range by the Swiss Federal Institute of Metrology, METAS (Guillevic et al., 2018). A suite of 11 primary standards was created using a technique that combines permeation tube substance loss determination by a magnetic suspension balance, dynamic dilution through mass flow controllers, and cryogenic collection in containers. These standards covered a range of 2.7–4.3 ppt. Comparison between assigned mole fractions and measured relative mole fractions against one of these primary standards revealed an internal consistency of this METAS-2017 calibration scale of 0.6 %. AGAGE adopted this calibration scale and all CFC-13 results reported here are on the METAS-2017 scale. A conversion factor of 1.05 for this METAS-2017 scale to the earlier interim calibration scale was determined.

Measurements of ΣCFC-114 and CFC-115 are reported on the SIO-05 primary calibration scales. They are defined through gravimetric preparations of 13 synthetic primary standards at ambient mole fraction levels prepared at SIO in 2005 (Prinn et al., 2000). They cover mole fraction ranges of 16–20 ppt for ΣCFC-114 and 8–10 ppt for CFC-115. Internal consistencies for these sets of standards of 0.14 % for ΣCFC-114 and 0.47 % for CFC-115 were estimated based on their relative results from inter-comparative measurements and their assigned relative mole fractions. Accuracies are initially estimated at 3 % (1σ) for each of the two CFCs, which is a conservative estimate based on previous experience with other compounds (a strict statistical treatment of the known uncertainties such as impurities, balance, etc., would likely lead to a much smaller overall uncertainty). For ΣCFC-114, there is a potential bias if our results of the combined isomer measurements were to be compared to the sum of their individual measurements (Supplement). Throughout this paper we report all our own measurements as dry-air mole fractions (substance fraction) in parts per trillion on these METAS and SIO calibration scales.

In some earlier articles (in particular Sturrock et al., 2001, 2002), ΣCFC-114 and CFC-115 measurements were published on calibration scales that were based on diluted, commercially obtained (Linde) high-concentration standards and were referred to as "UB" or "SIO-interim" calibration scales. A later revision resulted in a renaming of these calibration scales to UB-98B for measurements conducted at CSIRO and Cape Grim. After the creation of the SIO-05 primary calibration scales, SIO-05 / UB-98B conversion factors of 0.9565 for ΣCFC-114 and 1.0177 for CFC-115 were determined, with which UB-98B-based results need to be multiplied to determine their mole fraction on the SIO-05 calibration scales.

A comparison of the SIO-05 primary calibration scale for ΣCFC-114 with the UEA-2014 calibration scales (University of East Anglia, Laube et al., 2016) is of limited value and not straightforward because of the isomer issues addressed earlier. Nevertheless, for near-modern mole fractions (starting about mid-1990s, ∼ 16 ppt), numerically summed CFC-114 and CFC-114a mole fractions reported on the UEA-2014 calibration scales can be converted to SIO-05-reported ΣCFC-114 by multiplication of 1.025 (see Supplement).

2.6 Uncertainty assessment for reported measurements

To derive accuracies for the reported measurements we combine three independent uncertainties: uncertainties of the calibration scales mentioned in the previous subsection, a propagation uncertainty, and the instrumental precision of the measured sample, as listed in Sect. 2.4. The propagation uncertainties derive from the hierarchical sequence of standards used to propagate assigned mole fraction in the primary standards to the quaternary standards on-site by assuming measurement uncertainties for each of the steps, i.e., the secondary and tertiary standards. For this step, the measurement precisions are assumed to be the same as those of the quaternary standards on site. For ΣCFC-114 we add an "interference uncertainty", which is based on the findings of a potentially suppressed MS signal in the presence of *n*-butane (see Supplement). We estimate a maximum depletion of ΣCFC-114 of 0.6 % in the presence of 0.5 ppb *n*-butane (which we consider an upper limit in unpolluted air) and add this value as an independent uncertainty. For ΣCFC-114, there is also an earlier-mentioned potential isomer bias of ∼ 2 % with respect to the numeric sum of individual isomer measurements, which we include in our calculations. The resulting uncertainties (1σ) for the three compounds is then 3.7 % for CFC-13, 3.7 % for ΣCFC-114, and 3.2 % for CFC-115. They are dominated by the calibration scale uncertainties. For direct comparisons of samples reported on the same calibration scale, the calibration scale uncertainties do not apply and the remaining uncertainties are considerably smaller (2.2, 2.1, and 1.2 % for the three compounds).

2.7 Bottom-up inventory-based and other emission estimates

Here we refer to bottom-up emissions as those derived from data related to production, distribution, and usage of these compounds. For the CFCs discussed here such estimates have considerable uncertainties because of the large fraction of these CFCs installed in long-lasting equipment (banks) with unclear leakage rates. Nevertheless, bottom-up emission estimates are useful for us as prior for our model analysis and for comparison with our top-down observation-based results.

While bottom-up emissions are not available for CFC-13, they were published for ΣCFC-114 and CFC-115 from the refrigeration sector by Fisher and Midgley (1993). A more comprehensive set of emission estimates for these two compounds was released by AFEAS (Alternative Fluorocarbons Environmental Acceptability Study) for 1934–2003. For ΣCFC-114, they show an early onset of emissions in the 1930s with significant released quantities in the late 1940s

($\sim 7\,\mathrm{kt\,yr^{-1}}$) and peak emissions ($\sim 18\,\mathrm{kt\,yr^{-1}}$) in 1986/87. Extrapolation of the AFEAS data, as in Daniel and Velders (2007) (see Supplement), shows emissions of $< 0.1\,\mathrm{kt\,yr^{-1}}$ in the last few years and a remaining bank of 0.16 kt in 2016. On a similar basis, AFEAS CFC-115 bottom-up emissions started only in the mid-1960s and peaked in the early 1990s at $\sim 13\,\mathrm{kt\,yr^{-1}}$ before declining to $< 0.1\,\mathrm{kt\,yr^{-1}}$ from 2008, leaving a remaining bank of $< 0.01\,\mathrm{kt\,yr^{-1}}$ in 2016. Destruction of these two CFCs is considered insignificant in the AFEAS analysis; hence, the cumulative production matches the cumulative emissions. Some of these data were used in the Scientific Assessment of Ozone Depletion of 2006 to produce emission scenarios for 1930–2100 on which the atmospheric abundances for the same period were based (Daniel and Velders, 2007). Analogously, the AFEAS emission inventory for CFC-115 was also expanded into a scenario similar to ΣCFC-114, but these results were not graphically presented in the Scientific Assessment of Ozone Depletion. To facilitate public access to both the AFEAS original numerical data and those expanded in the Scientific Assessment of Ozone Depletion ("expanded AFEAS data"), we provide these in the Supplement, along with a description of how they were derived. These data are used in the present analysis as priors for the two global inversions.

We also compare our results with the data set derived by Velders and Daniel (2014), who reconstructed production, banks, and emissions for ΣCFC-114 and CFC-115, with projections into the future. Their reconstruction is a mix of bottom-up inventory-based and top-down observation-based data. The earlier parts of their records are largely based on the AFEAS results and therefore do not provide significant additional information. Those from 1979 to 2008 are based on atmospheric observations. Their ΣCFC-114 emissions after 2008 are based on a bank of 15 kt for that year. This bank was derived as a remnant of a 60 kt bank for 1960, which was back-extrapolated from emissions based on atmospheric observations and using a yearly emission factor (Daniel and Velders, 2011, G. J. M. Velders, personal communication, June 2017). For CFC-115, Velders and Daniel (2014) derived a bank of 15.9 kt from R-502 for 2008 (UNEP/TEAP, 2009, and unpublished data). The Velders and Daniel (2014) bank and emissions after 2008 are significantly larger than those from AFEAS for both compounds.

2.8 Firn model, global transport model, and inversions

Similar to the study by Vollmer et al. (2016) for halons, the present analysis uses a firn air model to characterize the age of the CFCs in the firn air samples (Trudinger et al., 2016), the AGAGE 12-box model to relate atmospheric mole fractions to surface emissions (Rigby et al., 2013), two inversion approaches to estimate hemispheric emissions, and a Lagrangian transport model to study regional emissions of CFC-115 in northeastern Asia.

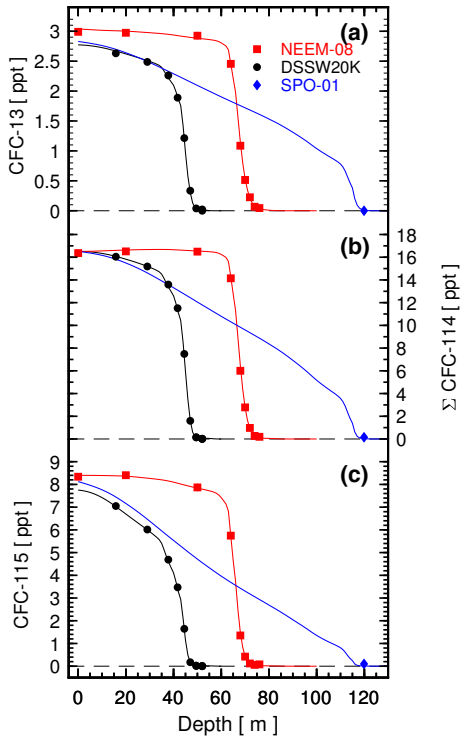

Figure 2. Depth profiles for the three chlorofluorocarbons CFC-13 **(a)**, ΣCFC-114 **(b)**, and CFC-115 **(c)** in polar firn. Measured dry-air mole fractions are shown for the Greenland site NEEM-08 (red squares) and the Antarctic sites Law Dome (DSSW20K, black circles) and South Pole (SPO-01, blue diamond). Generally the measurement precisions (1σ) are smaller than the plotting symbols. The modeled mole fraction depth profiles (solid lines) correspond to the optimized emission history from the CSIRO inversion, derived from the combined observations of all three firn sites, archived air, and in situ measurements.

2.8.1 Firn model

The firn model used here was developed at CSIRO by Trudinger et al. (1997) and updated by Trudinger et al. (2013). It has previously been used for firn air measurement reconstructions of other greenhouse gases (Sturrock et al., 2002; Trudinger et al., 2002, 2016; Vollmer et al., 2016). Physical processes in the firn, foremostly vertical diffusion, cause the air samples to represent age spectra rather than an individual discrete age as is found in tank samples like the CGAA. Green's functions are used to relate the measured mole fractions to the time range of the corresponding atmospheric mole fractions. The update to the firn model described in Trudinger et al. (2013) included a process that had previously been neglected by Trudinger et al. (1997). This process was the upward flow of air due to compression of the pore space as new snow accumulates above, and it appears that this process is important. As discussed in Trudinger et al. (2013), including it in the model removed a discrepancy be-

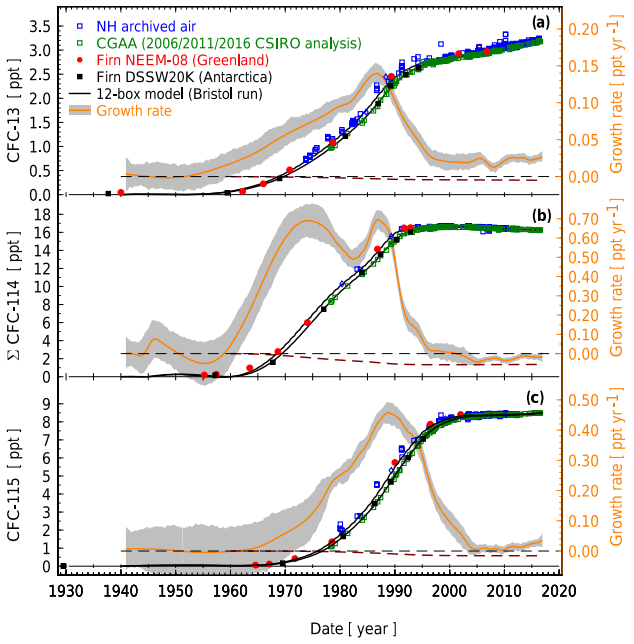

Figure 3. Measurements of the chlorofluorocarbons CFC-13 **(a)**, ΣCFC-114 **(b)**, and CFC-115 **(c)** from archived air samples and firn. Firn measurements are plotted against either effective or mean ages of the samples (see text). In situ measurement results from the AGAGE stations are not plotted for clarity. The inversion results are given for the Northern Hemisphere (upper solid lines) and Southern Hemisphere (lower solid lines). Growth rates (shown in orange using the right axes) are globally averaged from model results. Note that zero growth, shown as dashed black lines, is offset relative to the left axes. With focus on the recent part of the record the growth rates deviate significantly from the growth rates that would be obtained if zero emissions were assumed (shown as maroon dashed lines, calculated by dividing the global mole fraction by the lifetime).

tween DSSW20K firn and CGAA CFC-115 that was noted by Sturrock et al. (2002).

The diffusion coefficients used in this work for the three CFCs relative to CO_2 in air (for a temperature of 253 K) are 0.667 for CFC-13 (using Le Bas molecular volumes as described by Fuller et al., 1966), 0.495 for ΣCFC-114 (Matsunaga et al., 1993), and 0.532 for CFC-115 (Matsunaga et al., 1993). Measurement results and reconstructed firn air depth profiles are shown in Fig. 2. These modeled depth profiles are not based on the observations at the individual sites but rather correspond to the optimized emission history obtained using measurements from all firn sites as well as the atmospheric measurements used in this study. While ΣCFC-114 was present in all samples of the three sites, CFC-13 was absent within the detection limits in the South Pole sample and in one of the deepest duplicate samples at DSSW20K. CFC-115 was also absent in two of the three deepest DSSW20K duplicate samples.

2.8.2 AGAGE 12-box model

The AGAGE box model was originally created by Cunnold et al. (1983) and has since been rewritten and modified (Cunnold et al., 1994, 1997; Rigby et al., 2013; Vollmer et al., 2016). In the current version of the model, the atmosphere is divided into four zonal bands, separated at the Equator and at the 30° latitudes, thereby creating boxes of similar air masses. Boxes are also separated at altitudes represented by 500 and 200 hPa. Model transport parameters and stratospheric photolytic loss vary seasonally and repeat interannually (Rigby et al., 2013). For the CFCs analyzed here, loss in the atmosphere is dominated by photolytic destruction in the stratosphere. Here our local stratospheric loss rates are tuned to reflect the current best estimates of the global lifetimes of these compounds from SPARC (2013) as shown in Table 1.

Monthly transport parameters in the 12-box model were tuned to match the simulation of a uniformly distributed passive tracer in the Model for Ozone and Related Tracers (MOZART; Emmons et al., 2010), using Modern-Era Retrospective Analysis for Research and Application (MERRA) meteorology for the year 2000 (Rienecker et al., 2011). These transport parameters were repeated each year in our simulations. Whilst interannual variation in transport is known to impact the distribution of trace gases in the atmosphere, time-resolved atmospheric physical state estimates are not generally available throughout the entire period of this investigation. Furthermore, we anticipate that variations in emissions dominate atmospheric trends, particularly over the longer (multi-annual) timescales, which are our primary focus.

2.8.3 Global inversions

To estimate global emissions to the atmosphere we employ two different Bayesian inverse methods (Bristol and CSIRO). Both methods use the AGAGE 12-box model to relate observed tropospheric mole fractions to surface emissions of the CFCs. While past studies using the Bristol inversion have primarily targeted modern in situ observations from the AGAGE network (Rigby et al., 2011, 2014; Vollmer et al., 2011, 2015b; O'Doherty et al., 2014), the inversion method has also been extended to include firn air observations (Vollmer et al., 2016). Green's functions from the CSIRO firn model are used in both global inversions to relate the firn air measurements to atmospheric mole fraction over the appropriate time range.

The Bristol approach is based on the methods outlined in Rigby et al. (2011) and extended in Rigby et al. (2014). Briefly, this method assumes a constraint (prior) on the rate of change of emissions, which is adjusted using the data in a Bayesian framework. The magnitude of the uncertainty in the prior year-to-year emission growth rate is somewhat arbitrarily chosen to be 20 % of the maximum emission rate for the entire period. In a minor modification to the approach in Rigby et al. (2014), we chose to solve for a change in ab-

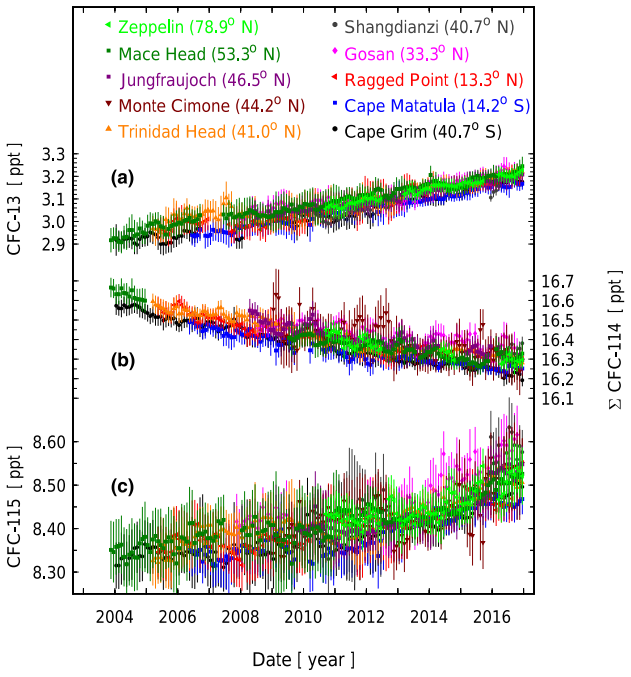

Figure 4. Abundances of the chlorofluorocarbons CFC-13 **(a)**, ΣCFC-114 **(b)**, and CFC-115 **(c)** at stations of the AGAGE (Advanced Global Atmospheric Gases Experiment) network. These in situ data are binned into monthly means after applying a pollution filter to limit the records to samples under background conditions (O'Doherty et al., 2001; Cunnold et al., 2002). Vertical bars are standard deviations of the monthly means (1σ). Occasional deviations of the Monte Cimone measurements from the other sites for ΣCFC-114 and CFC-115 (CFC-13 not measured at this site) are explained by the significantly larger propagation uncertainties (partially caused by larger precisions) for this site compared to the other site.

solute emissions ($\mathrm{kt\,yr^{-1}}$), rather than use a scaling of the prior emissions. This approach was found to lead to more consistent posterior emission uncertainty estimates between the near-zero and relatively high emission periods.

The random component of the model–measurement mismatch uncertainties in the Bristol inversion is composed of measurement uncertainties and those of the atmospheric and firn air models. The atmospheric model uncertainty is assumed to be equal to the variability in the estimated baseline within each monthly mean. These uncertainties are propagated through the model to provide a posterior emission uncertainty estimate (Rigby et al., 2014). The posterior emission uncertainty is then augmented with a term related to the calibration scale uncertainty and the uncertainty due to the lifetime (Rigby et al., 2014). The observations that are compared with the 12-box model in the Bristol inversion (see following section) are from all the firn air (firn model output) and CGAA archived air samples described here and the monthly mean background-filtered in situ measurements from Mace Head, Trinidad Head, Ragged Point, Cape Matatula, and Cape Grim (Fig. 4).

The CSIRO inversion, also combined with the 12-box model and Green's functions from the CSIRO firn model (Trudinger et al., 2016; Vollmer et al., 2016), was developed to focus on sparse observations from air archives and firn air and ice core samples that are associated with age spectra. The characteristics of these data necessitate the use of constraints on the inversion to avoid unrealistic oscillations in the reconstructed mole fractions or negative values of mole fraction or emissions. The CSIRO inversion therefore uses non-negativity constraints and favors relatively small changes to annual emissions in adjacent years rather than large, unrealistic fluctuations. A prior emission history based on bottom-up estimates is used as a starting point, then a nonlinear constrained optimization method is used to find the solution that minimizes a cost function consisting of the model–data mismatch plus the sum of the year-to-year changes in emissions (Trudinger et al., 2016). The observations used in the CSIRO inversion are the firn measurements and annual values of mole fraction from a smoothing spline fit to measurements at Cape Grim and the CGAA and another spline fit to Mace Head and the NH air archive. Uncertainties are estimated using a bootstrap method that incorporates data uncertainties and uncertainties in the firn model through the use of an ensemble of firn Green's functions.

We use the expanded AFEAS bottom-up inventory-based data for ΣCFC-114 and CFC-115 as prior in the inversions as these were produced without any input from atmospheric observations. For CFC-13, emission inventories do not exist to the best of our knowledge. As prior for this compound, we use the expanded CFC-115 AFEAS data, which we scale with a factor of 1/7 based on an intercomparison of production estimates (see Supplement).

2.8.4 Regional-scale source allocation and atmospheric inversion

Pollution events of the three compounds are absent, to within detection limits, from the measurements at all AGAGE field stations with the exception of Gosan (South Korea) and Shangdianzi (China). This has prompted a more detailed analysis of these compounds in northeastern Asia to locate and quantify potential sources. Only observations from Gosan were used since these are less locally influenced, and therefore less subject to sub-grid-scale model errors, than those from Shangdianzi, which are subject to pollution events originating in the nearby Beijing capital region.

We calculated qualitative emission distributions by combining model-derived source sensitivities with the baseline observations from Gosan above. A smooth statistical baseline fit (Ruckstuhl et al., 2012) was subtracted from the observational data. Surface source sensitivities were computed with the Lagrangian particle dispersion model FLEXPART (Stohl et al., 2005) driven by operational analysis and fore-

Table 2. By-country emissions of CFC-13, ΣCFC-114, and CFC-115, estimated by the regional inversion: prior and posterior estimates. Emissions from areas with HFC-125 factories are termed "hot spot". All values are given in units of $\mathrm{kt\,yr^{-1}}$; uncertainties represent a 1σ range.

Compound	Year	China		Hot spot		South Korea		Japan	
		Prior	Posterior	Prior	Posterior	Prior	Posterior	Prior	Posterior
CFC-13	2012	0.1 ± 0.045	0.14 ± 0.03	–	–	0.004 ± 0.004	0.001 ± 0.002	0.01 ± 0.008	0.007 ± 0.006
CFC-13	2013	0.1 ± 0.043	0.20 ± 0.03	–	–	0.004 ± 0.004	0.001 ± 0.002	0.01 ± 0.008	0.007 ± 0.005
CFC-13	2014	0.1 ± 0.043	0.15 ± 0.03	–	–	0.004 ± 0.004	0.003 ± 0.002	0.01 ± 0.008	0.007 ± 0.006
CFC-13	2015	0.1 ± 0.045	0.10 ± 0.03	–	–	0.004 ± 0.004	0.002 ± 0.002	0.01 ± 0.008	0.004 ± 0.006
CFC-13	2016	0.1 ± 0.045	0.10 ± 0.03	–	–	0.004 ± 0.004	0.001 ± 0.002	0.01 ± 0.008	0.004 ± 0.005
[1.5ex] ΣCFC-114	2012	0.4 ± 0.37	0.66 ± 0.23	–	–	0.015 ± 0.033	0.007 ± 0.008	0.04 ± 0.065	0.019 ± 0.026
ΣCFC-114	2013	0.4 ± 0.35	1.00 ± 0.24	–	–	0.015 ± 0.034	0.005 ± 0.005	0.04 ± 0.068	0.033 ± 0.029
ΣCFC-114	2014	0.4 ± 0.35	0.64 ± 0.21	–	–	0.015 ± 0.034	0.003 ± 0.006	0.04 ± 0.067	0.017 ± 0.027
ΣCFC-114	2015	0.4 ± 0.37	0.61 ± 0.17	–	–	0.015 ± 0.033	0.004 ± 0.007	0.04 ± 0.065	0.034 ± 0.036
ΣCFC-114	2016	0.4 ± 0.37	0.79 ± 0.23	–	–	0.015 ± 0.033	0.003 ± 0.008	0.04 ± 0.065	0.019 ± 0.034
[1.5ex] CFC-115	2012	0.2 ± 0.68	0.25 ± 0.36	0.018 ± 0.13	0.046 ± 0.039	0.007 ± 0.051	0.004 ± 0.008	0.02 ± 0.13	0.020 ± 0.066
CFC-115	2013	0.2 ± 0.62	0.68 ± 0.25	0.018 ± 0.13	0.28 ± 0.03	0.007 ± 0.053	0.002 ± 0.005	0.02 ± 0.12	0.029 ± 0.035
CFC-115	2014	0.2 ± 0.62	0.59 ± 0.26	0.016 ± 0.13	0.18 ± 0.04	0.007 ± 0.053	0.002 ± 0.006	0.02 ± 0.12	0.048 ± 0.038
CFC-115	2015	0.2 ± 0.68	0.78 ± 0.35	0.018 ± 0.13	0.080 ± 0.041	0.007 ± 0.051	0.002 ± 0.009	0.02 ± 0.12	0.015 ± 0.032
CFC-115	2016	0.2 ± 0.62	0.47 ± 0.41	0.018 ± 0.13	0.12 ± 0.06	0.007 ± 0.053	0.005 ± 0.008	0.02 ± 0.12	0.009 ± 0.029

casts from the European Centre for Medium-Range Weather Forecasts (ECMWF) Integrated Forecasting System (IFS) modeling system. For each 3-hourly time interval 50 000 model particles were released and followed backward in time for 10 days. Surface source sensitivities (concentration footprints) were obtained by evaluating the residence times of the model particles along the backward trajectories (Seibert and Frank, 2004).

Qualitative emission distributions were then calculated as a spatially distributed, weighted concentration average using the source sensitivities as weights. This method is based on the one described by Stohl (1996) for simple air mass trajectories but was generalized for source sensitivities and previously applied to halocarbon observations (Stemmler et al., 2007; Vollmer et al., 2015a). The method provides a general first impression of potential source locations but cannot be used to quantify individual sources and their uncertainty (location and length).

In addition, we applied a spatially resolved, regional-scale emission inversion using the same FLEXPART-derived source sensitivities and the Bayesian approach described in detail in Henne et al. (2016). In contrast to the method above, the Bayesian inversion provides a quantitative spatial distribution of posterior emissions and their uncertainties. Prior emissions were set proportional to the population density. The same emission factor per person was used for the entire inversion domain, which comprised most of China, North and South Korea, and the southwestern part of Japan. This emission factor was set in such a way that total Chinese emissions were in line with China's share of the gross world product of approximately 15 % and the global emission estimates described in Sect. 3.2.1, 3.2.4, and 3.2.6.

Parameters describing the covariance uncertainty matrices were derived from a log-likelihood maximum search (Michalak et al., 2005; Henne et al., 2016). The prior emission uncertainties obtained from this optimization were relatively large and amounted to 0.04, 0.4, and $0.6\,\mathrm{kt\,yr^{-1}}$ for China for CFC-13, ΣCFC-114, and CFC-115, respectively (see Table 2). All analysis was performed separately for each year from 2012 to 2016. More details on the applied method and additional results can be found in the Supplement.

3 Results and discussion

3.1 Atmospheric histories and high-resolution records

We combine our measurement results from firn air samples, archived air in canisters, and in situ measurements to produce the full historic records for CFC-13, ΣCFC-114, and CFC-115 spanning nearly 8 decades (Figs. 3–4). The modeled records discussed in this section derive from the Bristol and CSIRO inversions using these observations and the AGAGE 12-box model. The firn air depth profiles show a steady decline of all three CFCs with increasing depth (Fig. 2). All three compounds are at or below detection limits in the deepest samples of the Antarctic DSSW20K profile but clearly detectable in the deepest samples in the Greenland NEEM-2008 profile. These firn air results are plotted with the full historic record in Fig. 3 using dates based on the effective ages unless the mole fractions were near zero, when mean ages were used; note that these dates are used for graphical purposes only and that the full Green's functions (shown in the Supplement) were used in the inversions to represent the age of the compounds in firn air. On the temporal scale the firn air results overlap strongly with the results from the archived canisters. These canister samples span from the late 1970s to near present and overlap with the high-resolution in situ measurements shown in more detail in Fig. 4. The in situ data are binned into monthly means after applying a pol-

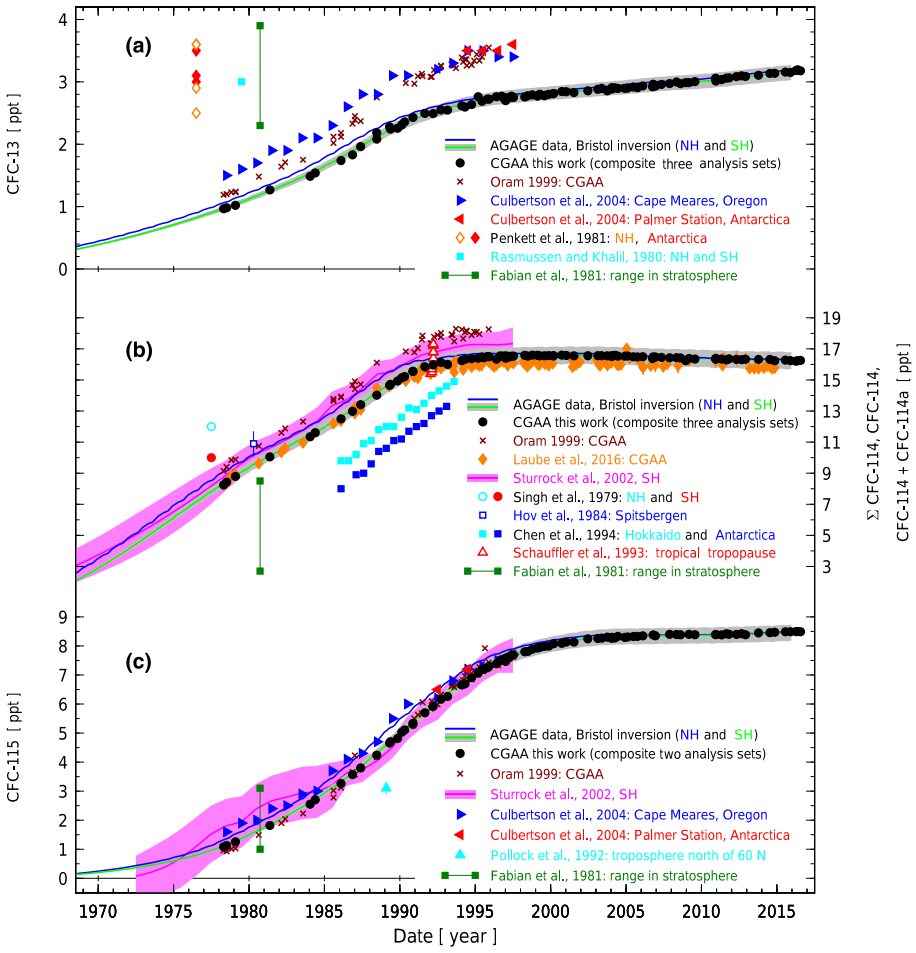

Figure 5. Comparison of the atmospheric records of CFC-13 **(a)**, ΣCFC-114 **(b)**, and CFC-115 **(c)** from this study with previous results. Cape Grim Air Archive (CGAA) samples and subsamples have been analyzed multiple times – here we show analysis results published by Oram (1999), Laube et al. (2016), and the present study (three separate analysis sets are averaged; see Supplement). Light grey bands denote the uncertainty on our SH model results including calibration uncertainty. Uncertainty bands for the NH, which are similar to the SH, are omitted from this plot for clarity. Results for ΣCFC-114 are from combined measurements of the two analytically unseparated $C_2Cl_2F_4$ isomers. Exceptions to this are the studies by Oram (1999) and Laube et al. (2016) in which the numerical sums of the two individual isomer measurements are shown. Also, results by Chen et al. (1994) (values approximated only from their graphical display) are of CFC-114 only. Assuming a 5–6 % contribution of CFC-114a in ΣCFC-114, these results are still significantly lower compared to our study. All results are left on the calibration scales of the published data.

lution filter to limit the records to samples under background conditions (O'Doherty et al., 2001; Cunnold et al., 2002).

3.1.1 CFC-13

CFC-13 first appeared in the atmosphere in the late 1950s to early 1960s (Fig. 3). Its growth rates were highest in the 1980s with a significant decline thereafter, presumably as a consequence of reduced emissions due to restrictions on production and consumption by the Montreal Protocol in the non-Article 5 countries. Because of its very long lifetime, small emissions are sufficient to maintain the observed increase in its abundance, and consequently CFC-13 continued to grow monotonically to a globally averaged mole fraction of 3.18 ppt in 2016. Its global growth rate leveled off in the late 1990s but has remained at a surprisingly high mean growth rate of 0.02 ppt yr^{-1} since 2000 with no indication of a further decline in the growth rate since then.

Cape Matatula and Cape Grim, which are the two stations most influenced by SH air masses, have shown a small and consistent offset of 0.04 ppt compared to the NH stations (SH lower), which points to predominantly NH emissions (Fig. 4). For the overlapping period of 1978–1997, our CFC-13 abundances are significantly lower (∼ 25 %) compared to earlier published data (Oram, 1999; Culbertson et al., 2004) (Fig. 5).

For most of the AGAGE field stations the high-resolution records show an absence of CFC-13 pollution events, indicat-

ing vanishing emissions within the local footprints of these stations. However, Gosan and Shangdianzi feature sporadic pollution events with abundances that reach up to ~ 6 ppt. Measurements from the urban sites Tacolneston (England), Dübendorf (Switzerland), and Aspendale (Australia, after removal of a nearby CFC-13 source in early 2010) show no pollution events, while those at La Jolla (USA) exhibit occasional pollution events, which, however, are smaller and less frequent than those at the two Asian field sites. High-resolution records are shown in the Supplement.

3.1.2 ΣCFC-114

ΣCFC-114 appeared in the atmosphere in the late 1950s to early 1960s at similar times to CFC-13 (Fig. 3). Its growth rate was highest in the 1970s and 1980s (0.5–0.8 ppt yr^{-1}) and declined strongly in the 1990s. ΣCFC-114 global mole fractions peaked in 1999–2002 at 16.6 ppt and have slightly declined since then to 16.3 ppt in 2016. Based on the data assimilated into the Bristol inversion framework, global growth rates have been negative since the early 2000s with a minimum at -0.04 ppt yr^{-1} (mean 2004–2006) but no indication of a further decline since then. A small interhemispheric gradient has been persisting over the last decades as is shown by the lower mole fractions for Cape Matatula and Cape Grim compared to the NH sites (Fig. 4).

Our SH ΣCFC-114 results exhibit lower mole fractions than those of Oram (1999) and those of Sturrock et al. (2002), who used a combination of the data from Oram (1999) and in situ AGAGE Cape Grim data from older instrumentation (Fig. 5). Also, our ΣCFC-114 abundances are significantly lower than those of Martinerie et al. (2009) for the records before 1980. In contrast, our CGAA mole fractions agree closely with the sum of the CFC-114 and CFC-114a mole fractions from Laube et al. (2016) in the older part of the record but become progressively higher (up to 2.5 %) for the modern part of the record compared to that reported by Laube et al. (2016).

The high-resolution records at the AGAGE field sites generally show no ΣCFC-114 pollution events, indicating vanishing emissions in the air mass footprints of these stations (see Supplement). The single exception is Gosan, which shows frequent pollution events reaching mole fractions of up to ~ 20 ppt (Shangdianzi data are hampered by an instrumental artifact and not further discussed here). The urban sites also exhibit a pattern as discussed for CFC-13 similar to Tacolneston, Dübendorf, and Aspendale featuring minor and infrequent pollution events, indicating that even in these urban areas emissions are small. However, the record at La Jolla shows very frequent pollution events with magnitudes of up to ~ 25 ppt. This can be caused by either a rather local source or more widespread emissions in the air mass footprint of this station. A more detailed analysis is beyond the scope of this study.

3.1.3 CFC-115

CFC-115 appeared in the atmosphere with a delay of nearly a decade compared to CFC-13 and ΣCFC-114. Its growth peaked at times similar to CFC-13 and the second maximum of ΣCFC-114, at rates of 0.4–0.5 ppt yr^{-1}. Its growth then slowed during the mid-2000s to near zero, with CFC-115 abundances leveling off at ~ 8.3 ppt in the late 1990s. However, surprisingly, the CFC-115 growth rate has increased since its minimum at 0.007 ppt yr^{-1} (mean 2004–2009) to ~ 0.026 ppt yr^{-1} (mean 2014–2016). This has caused an enhanced increase in the atmospheric abundances to 8.49 ppt in 2016, which is seen more clearly in the recent in situ measurements from the stations, with increases led by Northern Hemisphere sites (Fig. 4).

Our CFC-115 abundances agree well with earlier-published results by Culbertson et al. (2004), Oram (1999), Martinerie et al. (2009), and the younger part of the record by Sturrock et al. (2002), as is shown in Fig. 5. The latter study found somewhat larger mole fractions in the 1970s and 1980s, but this was mainly due to a process neglected in the old version of the CSIRO firn model (upward flow of air due to compression, as mentioned above). There are currently no other published data records covering the past 2 decades to which we could compare our results.

The high-resolution records at the AGAGE field sites show, similar to CFC-13 and ΣCFC-114, no pollution events, with the exception of a few rare and small excursions for some of the sites. Again, Gosan and Shangdianzi exhibit pollution events (typically up to 13 ppt), which have become more frequent since 2013 for Gosan, and are evident in the Shangdianzi record only starting in 2016 because of missing data for 2013–2016. The urban sites La Jolla and Dübendorf, particularly the former, exhibit pollution events with a more regular frequency. Aspendale showed CFC-115 pollution episodes mainly in 2006–2009 but to a much lesser degree in the most recent part of its record. CFC-115 pollution events are mostly absent from Tacolneston (see Supplement). These observations demonstrate that CFC-115 has not completely been removed from installed equipment in these urban areas.

3.2 Emissions

Global emissions of the three CFCs were calculated using the Bristol and CSIRO inversions covering nearly 8 decades and are shown in Fig. 6 for 1950 to 2016. For ΣCFC-114 and CFC-115, industry-based bottom-up and other reported emissions are available for comparison. For all three CFCs we find persistent lingering emissions in the past decades. While the emissions for CFC-13 and CFC-114 have remained stable (within uncertainties), those for CFC-115 have increased in recent years. In our discussion of these recent emissions we assume that other effects that could artificially create these lingering emissions, i.e., a slowdown of vertical

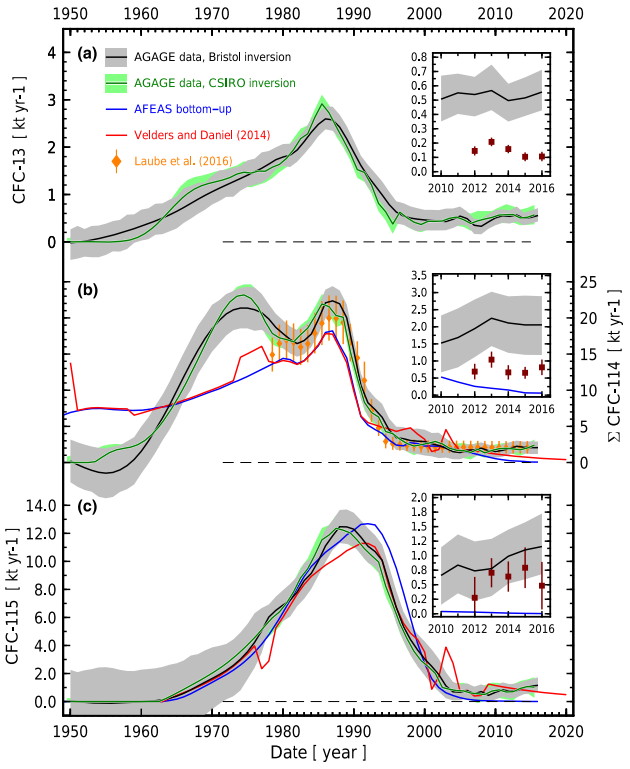

Figure 6. Global emissions of the chlorofluorocarbons CFC-13 **(a)**, ΣCFC-114 **(b)**, and CFC-115 **(c)** from atmospheric observations. Black lines and grey shaded areas are for the Bristol inversion and green lines and green shaded areas for the CSIRO inversion (see text). Emissions from Laube et al. (2016) are the sum of the emissions of both $C_2Cl_2F_4$ isomers. In the insets, our observation-based global emissions and the expanded AFEAS bottom-up emissions are compared to the East Asian emissions (maroon diamonds).

air mass exchange between the troposphere and the stratosphere and/or reduced removal fluxes, are absent. The global emission results are complemented with results for Asian regional emissions and with emissions found from specific processes (CFC-13) and compound impurities (CFC-115).

3.2.1 CFC-13 global emissions

Based on our inversions, CFC-13 emissions increased to a maximum of $\sim 2.6 \pm 0.25\,\mathrm{kt\,yr^{-1}}$ (1 SD) in the mid-1980s with a subsequent decline to relatively stable mean emissions of $0.48 \pm 0.15\,\mathrm{kt\,yr^{-1}}$ during the last decade (2007–2016, Fig. 6). Cumulative emissions until 2016 amount to 62 kt (both inversions), of which, due to its 640-year lifetime (Table 1), $\sim 90\,\%$ is still in the atmosphere. The persistent emissions over the past 2 decades are surprisingly high ($> 15\,\%$ of the peak emissions). The absence of a clear downward trend over this long period is inconsistent with a potential gradual replacement of CFC-13 in refrigeration units after the ban by the Montreal Protocol, which would lead to a decline of CFC-13 banks and emissions. Release functions for the other two CFCs used in the AFEAS vintage model (see Supplement) indicate that emissions of the whole charge of individual refrigeration equipment after installation take 20 years for ΣCFC-114 and 10 years for CFC-115. Assuming similar emission functions for CFC-13 in these applications could potentially explain the decline in the emissions in the 1990s but not the tailing emissions thereafter, about which we can only speculate. One explanation could be different release functions in the last 2 decades, for example a better containment for some time as a response to reduced availability of CFC-13 for refill, followed by a recent period of enhanced release perhaps due to intensified removal of old refrigeration equipment. Alternatively, CFC-13 could be emitted from sources other than refrigeration systems. It could be a by-product of fluorochemical manufacture and be released from the processes or as an impurity of the end products. It is unlikely that CFC-13 is used as a process agent as it would need to be recorded and controlled under the regulations of the Montreal Protocol, which is, as far as we know, not the case. The many CFC-13 pollution events measured at Shangdianzi and Gosan, and the rare occurrence at other sites, point to emissions in the East Asian region (although emissions may also be taking place in regions not seen by our high-frequency network).

3.2.2 CFC-13 emissions from regional FLEXPART inversion

The transport analysis of CFC-13 pollution peaks that were observed at Gosan did not reveal consistent and localized sources for the years 2012 to 2016. The strongest indication of sources was observed for 2013 and 2014 in China, whereas in 2015 and 2016 no specific source region could be identified (see Supplement). The Bayesian inversion showed relatively weak performance of the simulated prior time series (see Supplement) and the use of the posterior emission field did not improve these simulations to a large extent, with the exception of the year 2013, for which a considerable improvement of the simulation was achieved through the emission inversion. Consequently, the posterior emissions of CFC-13 stayed relatively close to the prior estimates, with the general tendency of lower posterior estimates for South Korea and Japan (Table 2, Fig. 7). Chinese emissions remained very close to the prior estimates except for the year 2013. In summary, these results do not indicate an overproportionate share of CFC-13 emissions from northeastern Asia compared with the global estimate and, considering the relatively weak model performance, are connected with a considerably large uncertainty.

3.2.3 CFC-13 emissions from aluminum smelters

CFC-13 was previously found in the emissions from aluminum plants (Harnisch, 1997; Penkett et al., 1981). Our present CFC-13 study has prompted us to reanalyze emission

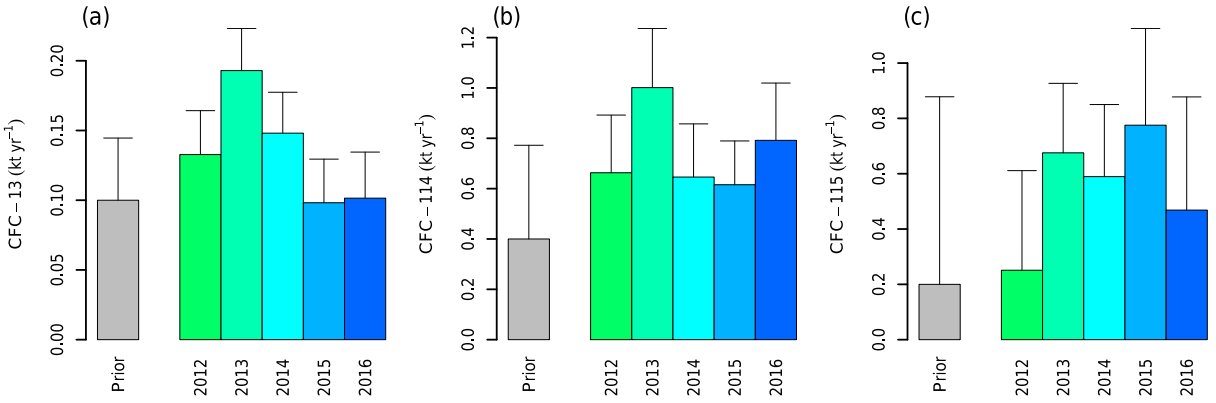

Figure 7. Total Chinese emissions of CFC-13 **(a)**, ΣCFC-114 **(b)**, and CFC-115 **(c)**, estimated with the regional inversion. Uncertainties represent a 1σ range.

measurements from an Australian aluminum smelter study (Fraser et al., 2013) (see Supplement). Contrary to what is stated in Fraser et al. (2013), that CFC-13 emissions were absent, our reanalysis revealed significant enhancement of CFC-13 in the exhaust samples compared to ambient air, thereby qualitatively confirming the results from the earlier studies. Enhancements over background levels of 45–130 ppt were found in the various smelter samples. From these results an emission factor of 0.025 ± 0.017 g CFC-13 per ton of aluminum was calculated. A global extrapolation based on a yearly aluminum production of $\sim 60\,\mathrm{Mt\,yr^{-1}}$ for 2016 (http://www.world-aluminium.org/statistics/#data, accessed June 2017) yields yearly CFC-13 emissions of $0.0015 \pm 0.001\,\mathrm{kt\,yr^{-1}}$. Unless emission factors from other smelters were significantly higher, this is suggestive of a minor contribution of aluminum smelter emissions to the total global yearly emissions of CFC-13 derived from our atmospheric observations. Nevertheless, from a chemical reaction standpoint, these CFC-13 emissions from aluminum production remain unexplained. Simplistically, since the carbon to produce CF_4 in aluminum smelters comes from the carbon in the smelter graphite anodes, chlorine impurities in the carbon anodes could be the source of chlorine to produce CFC-13 in the smelters.

3.2.4 ΣCFC-114 global emissions

Based on our global inversions, ΣCFC-114 emissions started in the 1950s–1960s and reached a maximum in the mid-1970s at $21 \pm 0.28\,\mathrm{kt\,yr^{-1}}$ followed by a second maximum in 1988 at $22 \pm 0.19\,\mathrm{kt\,yr^{-1}}$ (Fig. 6). Using the CSIRO inversion we have conducted a sensitivity analysis to investigate the robustness of this double peak. This has shown that the feature remains present when excluding each data set one at a time from the inversion; hence, it is not an artifact of the contribution from an individual data set (see Supplement). Global emissions declined strongly in the 1990s but remained at a surprisingly stable and high level at $1.9 \pm 0.84\,\mathrm{kt\,yr^{-1}}$ (mean of last decade, 2007–2016; see Fig. 6). Our global emissions differ significantly from the AFEAS bottom-up emissions for the first part of the record until about 1980. Bottom-up emissions are significantly elevated compared to our results until 1965 and are lower after that. Also, while we derive continuing emissions in the last decade, those from expanded AFEAS data sets were predicted to decline gradually to $< 0.1\,\mathrm{kt\,yr^{-1}}$ after 2014. Emissions of the last decade reported by Velders and Daniel (2014), which are derived in a bottom-up approach from assumed remaining banks, are higher than those from AFEAS but considerably smaller than the emissions we derived from our observations. Our estimates of the annual emissions for the recent years are large compared to the banks proposed by AFEAS (0.2 kt for 2016) and Velders and Daniel (2014) (6.4 kt for 2016) and are suggestive of additional, recently produced ΣCFC-114. Our cumulative emissions until 2016 (587 kt for the Bristol inversion and 586 kt for the CSIRO inversion) are higher than the cumulative emissions and productions derived by AFEAS from an inventory (521 kt) and those projected by Velders and Daniel (2014) (528 kt). However, despite this $\sim 10\,\%$ difference they agree within the large uncertainties, in particular those in the ΣCFC-114 lifetime (Table 1). Emissions derived by Laube et al. (2016) from atmospheric observations agree well with our emissions after 1980 but with some potential discrepancies in the earlier record (see Laube et al., 2016, for their full emission record).

We can only speculate on these relatively high lingering emissions of ΣCFC-114. One possible explanation is a change in release functions as was outlined for CFC-13. Alternatively, ΣCFC-114 could be fugitively emitted during synthesis of HFC-134a, where it is an intermediate compound in some synthesis pathways (Rao, 1994; Banks and Sharratt, 1996; McCulloch and Lindley, 2003). We have analyzed a diluted sample of HFC-134a from a container of the high-purity substance and found ΣCFC-114 present at $2.8 \times 10^{-5}\,\mathrm{mol\,mol^{-1}}$ of HFC-134a. If extrapo-

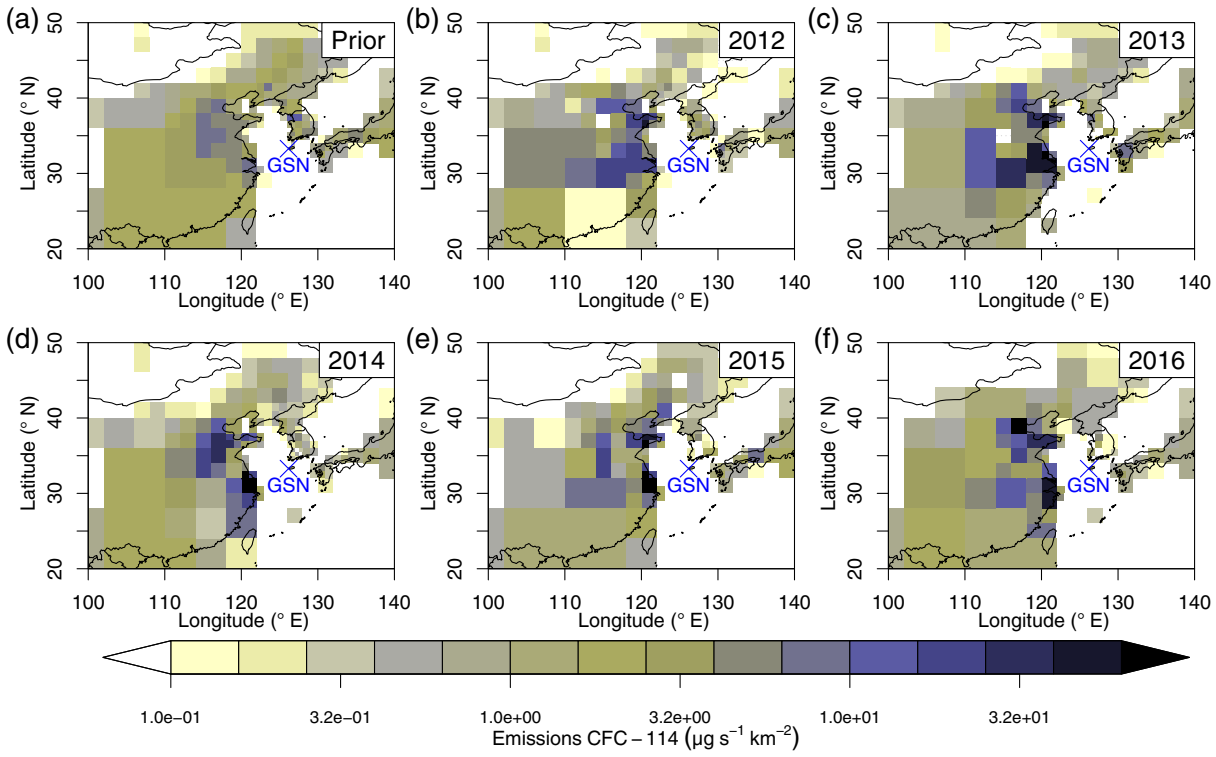

Figure 8. Emissions of ΣCFC-114 from northeastern Asia as estimated with inverse modeling using the ΣCFC-114 observations at Gosan (marked with a blue cross). **(a)** Common prior distribution; **(b–f)** posterior distribution for the years 2012 to 2016.

lated to global HFC-134a emissions of 180 kt yr^{-1} (Rigby et al., 2014) this would correspond to global emissions of 0.084 kt yr^{-1} of ΣCFC-114, which is a minor fraction of the current 1.9 kt yr^{-1}. A more comprehensive analysis would be necessary to obtain an understanding of the variability in such an impurity.

The observed latitudinal gradient in ΣCFC-114 abundance suggests predominant NH emissions. Pollution events in the Asian region, as detected from our high-resolution in situ measurements and the absence thereof in other regions suggest that at least some of these emissions originate from Asia. Increased abundances of CFC-114a, compared to Cape Grim, from samples collected in Taiwan were reported on by Laube et al. (2016), partially supporting our findings.

3.2.5 ΣCFC-114 emissions from regional FLEXPART inversion

In contrast to CFC-13, potential emission sources of ΣCFC-114 derived from our observations at Gosan could be identified on the Chinese mainland for the years after 2013 through the atmospheric transport analysis (see Supplement). The Bayesian regional inversion corroborates this finding, yielding largely increased posterior emissions for China for 2014 onward, with a peak of 1.0 ± 0.2 kt yr^{-1} in 2013 (Table 2, Fig. 7). South Korean and Japanese emissions remained around or below the prior values. Posterior emissions were mostly localized in two areas in China, in Shanghai and its neighboring provinces Zhejiang and Jiangsu and in Shandong Province (Fig. 8). The overall transport model performance and its improvement through the inversion (see Supplement) were considerably better in the case of CFC-13, lending sufficient confidence in the inversion results.

3.2.6 CFC-115 global emissions

Based on our inversions, CFC-115 emissions started in the mid-1960s and increased to a maximum of 12.5 ± 1.3 kt yr^{-1} in the late 1980s. Emissions declined strongly thereafter to a minimum of 0.59 ± 0.51 kt yr^{-1} (mean 2007–2010). Surprisingly the emissions have increased steadily since 2010 to 1.14 ± 0.50 kt yr^{-1} (mean 2015–2016), and the mean yearly emissions for the decade 2007–2016 were 0.80 ± 0.50 kt yr^{-1}. Our observations agree well with the bottom-up emissions by AFEAS except for an earlier maximum in our emissions, by a few years, compared to that by AFEAS, and except for our lingering and increasing emissions over the past years compared to vanishing emissions in the AFEAS record. Consequently, our cumulative emissions until 2016 of 243–245 kt (both inversions) agree well with the cumulative emissions and productions in the expanded AFEAS data of 237 kt and with those by Velders and Daniel (2014) of 228 kt, all within the large uncertainties of the CFC-115 lifetime (Table 1). Nevertheless, our annual emissions for the

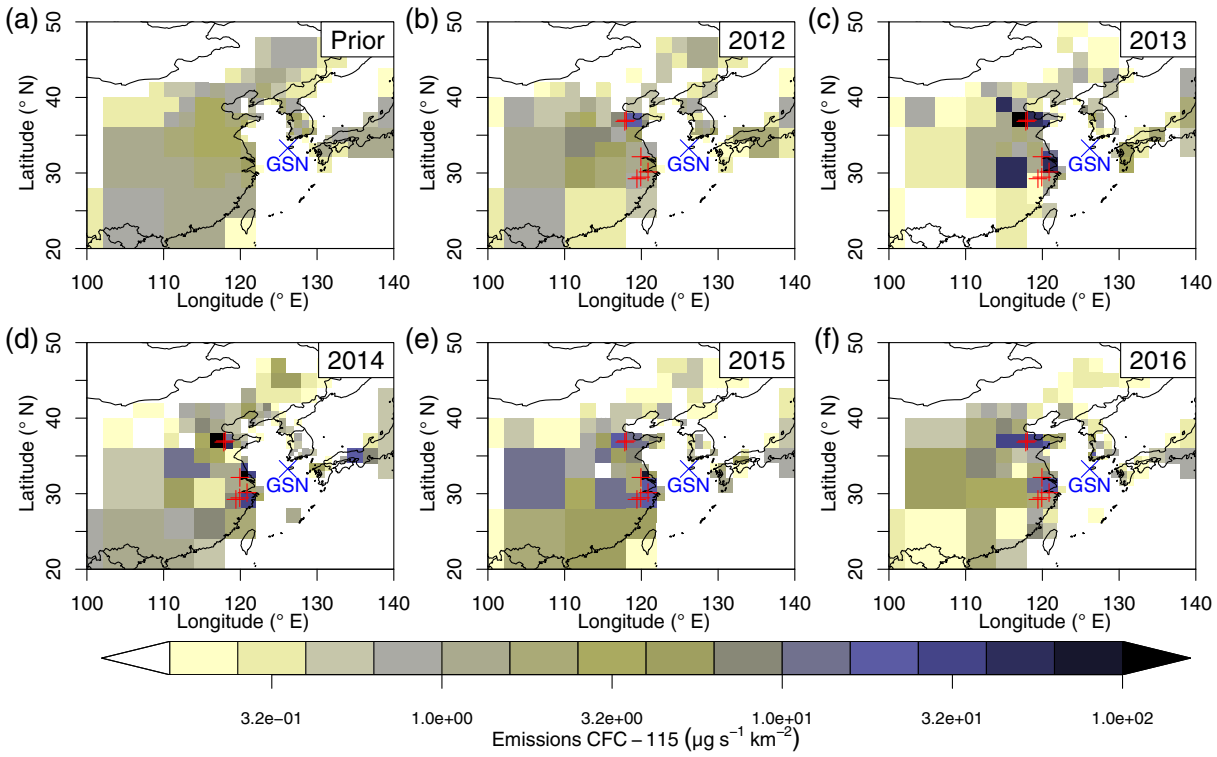

Figure 9. Emissions of CFC-115 from northeastern Asia as estimated with inverse modeling using the CFC-115 observations at Gosan (marked with a blue cross). **(a)** Common prior distribution; **(b–f)** posterior distribution for the years 2012 to 2016. Red plus signs mark the location of known HFC-125 factories, which are hypothesized to be potential sources of CFC-115.

recent years are large compared to the banks proposed by AFEAS (< 0.01 kt for 2016) and Velders and Daniel (2014) (8.6 kt for 2016) and are suggestive of additional, recently produced CFC-115.

3.2.7 CFC-115 emissions from regional FLEXPART inversion

The transport analysis of CFC-115 pollution peaks that were observed at Gosan indicated potential emission sources to be mainly located on the Chinese mainland (see Supplement). For the year 2012, no strong sources were located in the domain. Thereafter, potential source locations were identified in the larger Shanghai area (years 2013–2015) and more diffusely from a broad area along the eastern Chinese coast (year 2016). Similarly, the Bayesian inversion yielded increases in posterior emissions mostly located within two areas in eastern China (Fig. 9), the larger Shanghai area (including Zhejiang and Jiangsu provinces) and the northern part of the Shandong province. Large posterior emissions were detected for all analyzed years with the most prominent emissions in 2013 and 2014 and smaller posterior emissions in 2012. The locations of increased posterior emissions largely agree with the location of HFC-125 factories (B. Yao, personal communication, 2017), which we speculate are sources of CFC-115 emissions (see below) and which were not used in the prior. Large posterior emissions in other parts of the domain were not robust, varied from year to year, and were also connected with large posterior uncertainties. Total Chinese CFC-115 emissions were estimated to average 0.63 ± 0.32 kt yr^{-1} for the years 2013 to 2016 (Table 2, Fig. 7), whereas they remained relatively close to the prior value in 2012 (0.25 ± 0.36 kt yr^{-1}). The contribution of those grid cells containing the HFC-125 factories to the total Chinese emissions was considerably increased in the posterior estimates and reached between 12 and 41 %, whereas they only contributed 9 % in the prior. Posterior estimates for Japan and South Korea did not increase compared to the prior emission estimates.

3.2.8 CFC-115 emissions from HFC-125 production and use

We hypothesize that the increased CFC-115 emissions derive, at least in part, from the production of hydrofluorocarbons (HFCs), which have been produced in large quantities during the last 2 decades. Similar hypotheses were recently put forward for emissions of other CFCs and HCFCs. HCFC-133a (Laube et al., 2014; Vollmer et al., 2015c) and CFC-114a (Laube et al., 2016) emissions were speculated to derive, at least in part, from the production of HFC-134a, and HCFC-31 was speculated to derive from the produc-

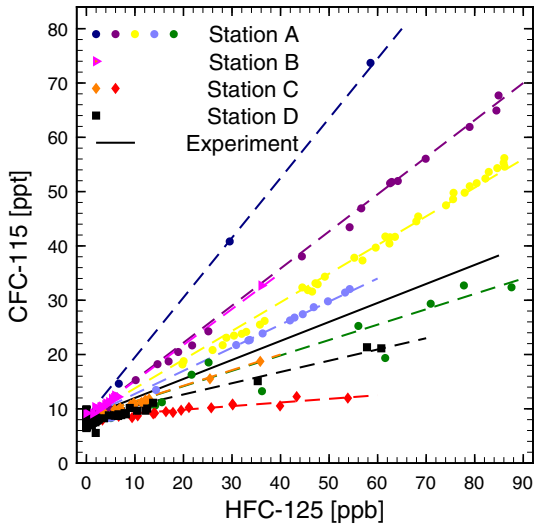

Figure 10. CFC-115 contamination in HFC-125 as found in contaminated laboratory air samples at AGAGE stations. Measurements are shown for four stations (A–D) during times of air conditioner leakages (R-410, 50–55 % by mass HFC-125, rest is HFC-32). They are plotted for a HFC-125 range of 0–90 ppb (parts per billion, 10^{-9}). Differently colored episodes are separated by times of air conditioner maintenance and refilling, demonstrating the variable fraction of CFC-115 in differing batches of the refrigerant. Based on these observations we find a range from 0.7×10^{-4} mol to 11×10^{-4} mol CFC-115/mol HFC-125. The solid line (3.5×10^{-4} mol CFC-115/mol HFC-125) is the result from a direct measurement of CFC-115 in a dilution of an independently obtained sample of pure HFC-125. Dashed lines are approximated only and serve as visual support of the data.

tion of HFC-32 (Schoenenberger et al., 2015). The most likely candidate, in the case of CFC-115, is the synthesis of the refrigerant HFC-125. CFC-115 is a known byproduct in one possible pathway to synthesize HFC-125, where tetrachloroethylene is treated with hydrogen fluoride (Rao, 1994; Shanthan Rao et al., 2015) followed by fluorine and chlorine exchanges. Although this pathway is not expected to be widely applied (A. McCulloch, personal communication, 2017) there are nevertheless 4 out of 12 production facilities in China using this method (Chinese Chemical Investment Network, 2017). A possible source is the leakage of CFC-115 to the atmosphere as an intermediate product at the factory level, similar to the speculations put forward in the studies above. However, this hypothesis is difficult to test without factory-level measurements because uncertainties in the localization of "hot spot" emissions, such as the one identified with our regional modeling, exceed the narrow geographical location of a factory potentially present in the area. Nevertheless, our analysis of regional emissions agrees with this hypothesis.

In addition to potential CFC-115 emissions at the HFC-125 factory level, we tested the hypothesis of CFC-115 impurities in HFC-125, which would then be emitted to the atmosphere during leakage of HFC-125 in installed refrigeration equipment. HFC-125 and CFC-115 have similar physicochemical properties, making it technically difficult to separate the two compounds (Corbin and Reutter, 1997; Kohno and Shibanuma, 2001; Brandstater et al., 2003; Cuzzato and Peron, 2003; Azzali and Basile, 2004; Piepho et al., 2006). We have detected CFC-115 in dilutions of high-purity HFC-125 (Fig. 10). We have also found excess (above ambient) CFC-115 in laboratory air at AGAGE sites at times of air conditioner leakage (Fig. 10). Excess CFC-115 correlated strongly with the main constituents of the air conditioners (R-410, 50–55 % by mass HFC-125, rest HFC-32), but ratios varied depending on site and recharge batch of the air conditioner fluid. These measurements have enabled us to demonstrate impurities ranging from 0.7 to 11×10^{-4} mol CFC-115/mol HFC-125. We extrapolate these to global CFC-115 emissions based on this range, and using estimates of global HFC-125 emissions (40 kt yr^{-1}; Rigby et al., 2014), we conclude that this impurity source accounts for only 0.0036–0.057 kt yr^{-1}. These impurity-based emissions are significantly below the last decade's (2007–2016) mean yearly emissions of 0.80 kt yr^{-1} derived from our inversions and they are also much lower than the recent growth in the CFC-115 global emissions. Note that HFC-125 in polluted air advected to the sites is generally too low to detect a corresponding CFC-115 enhancement; hence, we cannot extend this CFC-115 / HFC-125 ratio analysis to the regular air measurements. The CFC-115 / HFC-125 ratios in the CFC-115 pollution events observed at Gosan largely exceed the ratios found from air conditioner leakage, thereby indicating sources other than HFC-125 impurities.

4 Conclusions

Based on a wealth of new observations, we reconstruct the atmospheric histories of CFC-13, ΣCFC-114, and CFC-115 from their first appearance in the atmosphere to 2016. This is the first comprehensive study of very-long-lived CFC-13 in the atmosphere. We show that growth rates for CFC-13 (> zero) and ΣCFC-114 (< zero) have not declined for at least the last decade. For CFC-115, model results are suggestive of an increase in the growth rates in recent years. These observations make CFC-13 and CFC-115 two of the few CFCs left with increasing global atmospheric abundances. Under the assumptions of no significant change in global atmospheric transport patterns or sink processes, these growth rates correspond to ongoing emissions, which have remained stable or even increased (in the case of CFC-115) over the past decade. This contrasts with the expectations of declining emissions due to the phase-out of these compounds under the regulations of the Montreal Protocol. We provide evidence for small emissions of ΣCFC-114 and CFC-115 as impurities in HFCs and speculate on the possibility of fugitive emissions at the process level. We also find evidence

of small emissions of CFC-13 from aluminum smelting, but the chemistry that leads to CFC-13 production is not obvious. Impurities and fugitive emissions are not regulated by the Montreal Protocol; however, even if these are small emissions, they can potentially lead to an increasing atmospheric abundance, particularly for the long-lived CFC-13. For ΣCFC-114 and CFC-115, we find significant emissions from the Asian region but the processes responsible remain largely unknown.

Data availability. Data used in this study are available from the Supplement, from https://agage.mit.edu/, and from data repositories referenced therein.

The Supplement related to this article is available online at https://doi.org/10.5194/acp-18-979-2018-supplement.

Competing interests. The authors declare that they have no conflict of interest.

Acknowledgements. We acknowledge the station personnel at all stations for their continuous support in conducting in situ measurements and in flask sampling at Cape Grim (CSIRO and Bureau of Meteorology) and King Sejong (KOPRI). David Oram (UEA) is acknowledged for analytic CFC-114a/CFC-114 details of an SIO primary standard and James Burkholder for clarifications on the CFC-114 climate metrics. The joint Cape Grim Air Archive (CGAA) project is operated by CSIRO and the Australian Bureau of Meteorology. AGAGE operations are supported by NASA with grants NAG5-12669, NNX07AE89G, NNX11AF17G, and NNX16AC98G to MIT and grants NNX07AE87G, NNX07AF09G, NNX11AF15G, and NNX11AF16G to SIO. Further support comes from the Department for Business, Energy & Industrial Strategy (BEIS) contract 1028/06/2015 to the University of Bristol for Mace Head and the University of East Anglia for Tacolneston and NOAA (USA) contract RA-133-R15-CN-0008 to the University of Bristol for Barbados. Support for the Australian operations also comes from the Commonwealth Scientific and Industrial Research Organization (CSIRO Australia), the Bureau of Meteorology (Australia), the Department of Environment and Energy (Australia), and Refrigerant Reclaim Australia. Financial support for the measurements at the other sites is provided for Jungfraujoch by the Swiss National Program HALCLIM (Swiss Federal Office for the Environment, FOEN) and by the International Foundation High Altitude Research Stations Jungfraujoch and Gornergrat (HFSJG); for Zeppelin by the Norwegian Environment Agency; for Monte Cimone by the National Research Council of Italy and the Italian Ministry of Education, University and Research through the Project of National Interest Nextdata; for Gosan by the Korea Meteorological Administration research and development program under grant CATER 2014-6020; and for Shangdianzi by the National Nature Science Foundation of China (41575114). Support for King Sejong flask samples comes from the Swiss State Secretariat for Education and Research and Innovation (SERI), the National Research Foundation of Korea for the Korean–Swiss Science and Technology Cooperation Program, and the Korean Polar Research Institute programs PE13410 and PP16102. CSIRO's contribution was supported in part by the Australian Climate Change Science Program (ACCSP), an Australian government initiative. Australian firn activities in the Antarctic are specifically supported by the Australian Antarctic Science Program. We acknowledge the members of the firn air sampling teams for provision of the samples from Law Dome, NEEM, and South Pole. NEEM is directed and organized by the Center of Ice and Climate at the Niels Bohr Institute and US NSF, Office of Polar Programs. It is supported by funding agencies and institutions in Belgium (FNRS-CFB and FWO), Canada (NRCan/GSC), China (CAS), Denmark (FIST), France (IPEV, CNRS/INSU, CEA, and ANR), Germany (AWI), Iceland (RannIs), Japan (NIPR), Korea (KOPRI), the Netherlands (NWO/ALW), Sweden (VR), Switzerland (SNF), the UK (NERC), and the USA (US NSF, Office of Polar Programs). Martin K. Vollmer acknowledges a 2011 CSIRO Office of the Chief Executive Distinguished Visiting Scientist grant, and 2016 grants from Empa and SNF to CSIRO Aspendale for technical development and archived air and firn air measurements. Matthew Rigby was supported in part by advanced research fellowships from the UK Natural Environment Research Council (NERC, NE/1021365/1).

Edited by: Neil M. Donahue
Reviewed by: two anonymous referees

References

Azzali, D. and Basile, G.: Purification process of pentafluoroethane (HFC-125), EP Patent 1 153 907, available at: https://www.google.com/patents/EP1153907B1?cl=un (last access: 6 December 2017), 2004.

Baasandorj, M., Feierabend, K. J., and Burkholder, J. B.: Rate coefficients and ClO radical yields in the reaction of $O(^1D)$ with $CClF_2CCl_2F$, CCl_3CF_3, $CClF_2CClF_2$, and CCl_2FCF_3, Int. J. Chem. Kinet., 43, 393–401, https://doi.org/10.1002/kin.20561, 2011.

Baasandorj, M., Fleming, E. L., Jackman, C. H., and Burkholder, J. B.: $O(^1D)$ kinetic study of key ozone depleting substances and greenhouse gases, J. Phys. Chem. A, 117, 2434–2445, https://doi.org/10.1021/jp312781c, 2013.

Banks, R. E. and Sharratt, P. N.: Environmental Impacts of the Manufacture of HFC-134a, Tech. rep., Department of Chemistry and Department of Chemical Engineering, UMIST, Manchester, 1996.

Brandstater, S. M., Cohn, M., Hedrick, V. E., and Iikubo, Y.: Processes for purification and production of fluorocarbons, US Patent App. 10/075 560, available at: https://www.google.ch/patents/US20030164283 (last access: 6 December 2017), 2003.

Buizert, C., Martinerie, P., Petrenko, V. V., Severinghaus, J. P., Trudinger, C. M., Witrant, E., Rosen, J. L., Orsi, A. J., Rubino, M., Etheridge, D. M., Steele, L. P., Hogan, C., Laube, J. C., Sturges, W. T., Levchenko, V. A., Smith, A. M., Levin, I., Conway, T. J., Dlugokencky, E. J., Lang, P. M., Kawamura, K.,

Jenk, T. M., White, J. W. C., Sowers, T., Schwander, J., and Blunier, T.: Gas transport in firn: multiple-tracer characterisation and model intercomparison for NEEM, Northern Greenland, Atmos. Chem. Phys., 12, 4259–4277, https://doi.org/10.5194/acp-12-4259-2012, 2012.

Burkholder, J. B. and Mellouki, W.: Evaluation of atmospheric loss processes, in: SPARC Report on the Lifetimes of Stratospheric Ozone-Depleting Substances, Their Replacements, and Related Species, Chapter 1, 6, WCRP-15/2013, available at: http://www.sparc-climate.org/publications/sparc-reports/sparc-report-no6/ (last access: 6 December 2017), 2013.

Butler, J. H., Montzka, S. A., Battle, M., Clarke, A. D., Mondeel, D. J., Lind, J. A., Hall, B. D., and Elkins, J. W.: Collection and Analysis of Firn Air from the South Pole, 2001, AGU Fall Meeting Abstracts, p. F145, 2001.

Calm, J. M. and Hourahan, G. C.: Physical, safety, and environmental data for current and alternative refrigerants, in: Refrigeration for Sustainable Development, Proceedings of the 23rd International Congress of Refrigeration (ICR 2001), International Institute of Refrigeration (IRR/IFF), Prague, Czech Republic, 21–26 August 2001, 2011.

Carpenter, L. J. and Reimann, S.: Ozone-Depleting Substances (ODSs) and other gases of interest to the Montreal Protocol, in: Scientific Assessment of Ozone Depletion: 2014, Global Ozone Research and Monitoring Project — Report No. 55, Chapter 1, World Meteorological Organisation, Geneva, Switzerland, 2014.

Chen, L., Makide, Y., and Tominaga, T.: Determination of 1,2-dichlorotetrafluoroethane (CFC-114) concentration in the atmosphere, Chem. Lett., 571–574, https://doi.org/10.1246/cl.1994.571, 1994.

Chinese Chemical Investment Network, 2017: Chinese Chemical Investment Network and Shanghai Liujian Investment Consultants Limited: Technic and Market Research Report of HFC-125 (2011), available at: https://wenku.baidu.com/view/a75999bdfd0a79563c1e72a5.html, last access: 31 August 2017 (in Chinese).

Clerbaux, C. and Cunnold, D. M.: Long-lived compounds, in: Scientific Assessment of Ozone Depletion: 2006, Global Ozone Research and Monitoring Project, Report No. 50, Chapter 1, World Meteorological Organization, Geneva, Switzerland, 572 pp., 2007.

Corbin, D. R. and Reutter, D. W.: Purifaction of pentafluoroethanes, US Patent 5 648 569, available at: http://www.google.ch/patents/US5648569 (last access: 6 December 2017), 1997.

Culbertson, J. A., Prins, J. M., Grimsrud, E. P., Rasmussen, R. A., Khalil, M. A. K., and Shearer, M. J.: Observed trends for CF_3-containing compounds in background air at Cape Meares, Oregon, Point Barrow, Alaska, and Palmer Station, Antarctica, Chemosphere, 55, 1109–1119, https://doi.org/10.1016/j.chemosphere.2003.11.002, 2004.

Cunnold, D. M., Prinn, R. G., Rasmussen, R. A., Simmonds, P. G., Alyea, F. N., Cardelino, C. A., Crawford, A. J., Fraser, P. J., and Rosen, R. D.: The atmospheric lifetime experiment 3. Lifetime methodology and application to 3 years of $CFCl_3$ data, J. Geophys. Res., 88, 8379–8400, https://doi.org/10.1029/JC088iC13p08379, 1983.

Cunnold, D. M., Fraser, P. J., Weiss, R. F., Prinn, R. G., Simmonds, P. G., Miller, B. R., Alyea, F. N., and Crawford, A. J.: Global trends and annual releases of CCl_3F and CCl_2F_2 estimated from ALE/GAGE and other measurements from July 1978 to June 1991, J. Geophys. Res., 99, 1107–1126, https://doi.org/10.1029/93JD02715, 1994.

Cunnold, D. M., Weiss, R. F., Prinn, R. G., Hartley, D., Simmonds, P. G., Fraser, P. J., Miller, B., Alyea, F. N., and Porter, L.: GAGE/AGAGE measurements indicating reductions in global emissions of CCl_3F and CCl_2F in 1992–1994, J. Geophys. Res., 102, 1259–1269, https://doi.org/10.1029/96JD02973, 1997.

Cunnold, D. M., Steele, L. P., Fraser, P. J., Simmonds, P. G., Prinn, R. G., Weiss, R. F., Porter, L. W., O'Doherty, S., Langenfelds, R. L., Krummel, P. B., Wang, H. J., Emmons, L., Tie, X. X., and Dlugokencky, E. J.: In situ measurements of atmospheric methane at GAGE/AGAGE sites during 1985–2000 and resulting source inferences, J. Geophys. Res., 107, 4225, https://doi.org/10.1029/2001JD001226, 2002.

Cuzzato, P. and Peron, S.: Process for purifying pentafluoroethane from chloropentafluoroethane, US Patent 6 512 150, available at: https://www.google.ch/patents/US6512150 (last access: 6 December 2017), 2003.

Daniel, J. S. and Velders, G. J. M.: Halocarbon scenarios, ozone depletion potentials, and global warming potentials, in: Scientific Assessment of Ozone Depletion: 2006, Global Ozone Research and Monitoring Project, Report No. 50, Chapter 8, World Meteorological Organization, Geneva, Switzerland, 572 pp., 2007.

Daniel, J. S. and Velders, G. J. M.: A focus on information and options for policymakers, in: Scientific Assessment of Ozone Depletion: 2010, Global Ozone Research and Monitoring Project, Report No. 52, Chapter 5, World Meteorological Organisation, Geneva, Switzerland, 2011.

Davis, M. E., Bernard, F., McGillen, M. R., Fleming, E. L., and Burkholder, J. B.: UV and infrared absorption spectra, atmospheric lifetimes, and ozone depletion and global warming potentials for CCl_2FCCl_2F (CFC-112), CCl_3CClF_2 (CFC-112a), CCl_3CF_3 (CFC-113a), and CCl_2FCF_3 (CFC-114a), Atmos. Chem. Phys., 16, 8043–8052, https://doi.org/10.5194/acp-16-8043-2016, 2016.

Emmons, L. K., Walters, S., Hess, P. G., Lamarque, J.-F., Pfister, G. G., Fillmore, D., Granier, C., Guenther, A., Kinnison, D., Laepple, T., Orlando, J., Tie, X., Tyndall, G., Wiedinmyer, C., Baughcum, S. L., and Kloster, S.: Description and evaluation of the Model for Ozone and Related chemical Tracers, version 4 (MOZART-4), Geosci. Model Dev., 3, 43–67, https://doi.org/10.5194/gmd-3-43-2010, 2010.

Fabian, P., Borchers, R., Penkett, S. A., and Prosser, N. J. D.: Halocarbons in the stratosphere, Nature, 294, 733–735, https://doi.org/10.1038/294733a0, 1981.

Fabian, P., Borchers, R., Krüger, B. C., and Lal, S.: The vertical distribution of CFC-114 ($CClF_2$-$CClF_2$) in the atmosphere, J. Geophys. Res., 90, 13091–13093, https://doi.org/10.1029/JD090iD07p13091, 1985.

Fabian, P., Borchers, R., Leifer, R., Subbaraya, B. H., Lal, S., and Boy, M.: Global stratospheric distribution of halocarbons, Atmos. Environ., 30, 1787–1796, https://doi.org/10.1016/1352-2310(95)00387-8, 1996.

Fisher, D. A. and Midgley, P. M.: The production and release to the atmosphere of CFCs 113, 114 and 115, Atmos. Environ., 27A, 271–276, https://doi.org/10.1016/0960-1686(93)90357-5, 1993.

Fraser, P. J., Langenfelds, R. L., Derek, N., and Porter, L. W.: Studies in Archiving Techniques, vol. 1989, Department of the Arts,

Sport, the Environment, Tourism and Territories, Bureau of Meteorology and CSIRO Division of Atmospjeric Research, Canberra, Australia, 16–29, 1991.

Fraser, P., Steele, P., and Cooksey, M.: PFC and carbon dioxide emissions from an Australian aluminium smelter using time-integrated stack sampling and GC-MS, GC-FID analysis, in: Light Metals 2013, edited by: Sadler, B. A., John Wiley and Sons, Inc., Hoboken, NJ, USA, 871–876, https://doi.org/10.1002/9781118663189.ch148, 2013.

Fraser, P. J. Steele, L. P., Pearman, G. I., Coram, S., Derek, N., Langenfelds, R. L., and Krummel, P. B.: Non-Carbon Dioxide Greenhouse Gases at Cape Grim: A 40 Year Odyssey, vol. 2016, Bureau of Meteorology and CSIRO Oceans and Atmosphere, Melbourne, Australia, 45–76, 2016.

Fuller, E. N., Schettler, P. D., and Giddings, J. C.: A new method for prediction of binary gas-phase diffusion coefficients, Ind. Eng. Chem., 58, 19–27, 1966.

Guillevic, M., Vollmer, M. K., Wyss, S. A., Leuenberger, D., Ackermann, A., Pascale, C., Niederhauser, B., and Reimann, S.: Dynamic-gravimetric preparation of metrologically traceable primary calibration standards for halogenated greenhouse gases, in preparation, 2018.

Harnisch, J.: Die Globalen Atmosphärischen Haushalte der Spurengase Tetrafluormethan (CF_4) und Hexafluorethan (C_2F_6), PhD Thesis, University of Göttingen, Cuvillier, Göttingen, Germany, 1997.

Harris, N. R. P. and Wuebbles, D. J.: Scenarios and information for policymakers, in: Scientific Assessment of Ozone Depletion: 2014, Global Ozone Research and Monitoring Project, Report No. 55, Chapter 5, World Meteorological Organisation, Geneva, Switzerland, 2014.

Henne, S., Brunner, D., Oney, B., Leuenberger, M., Eugster, W., Bamberger, I., Meinhardt, F., Steinbacher, M., and Emmenegger, L.: Validation of the Swiss methane emission inventory by atmospheric observations and inverse modelling, Atmos. Chem. Phys., 16, 3683–3710, https://doi.org/10.5194/acp-16-3683-2016, 2016.

Hodnebrog, Ø., Etminan, M., Fuglestvedt, J. S., Marston, G., Myhre, G., Nielsen, C. J., Shine, K. P., and Wallington, T. J.: Global warming potentials and radiative efficiencies of halocarbons and related compounds: a comprehensive review, Rev. Geophys., 51, 300–378, https://doi.org/10.1002/rog.20013, 2013.

Hov, Ø., Penkett, S. A., Isaksen, I. S. A., and Semb, A.: Organic gases in the Norwegian Arctic, Geophys. Res. Lett., 11, 425–428, https://doi.org/10.1029/GL011i005p00425, 1984.

IPCC/TEAP: Special Report on Safeguarding the Ozone Layer and the Global Climate System: Issues Related to Hydrofluorocarbons and Perfluorocarbons. Prepared by Working Group I and III of the Intergovernmental Panel on Climate Change, and the Technology and Economic Assessment Panel, Cambridge University Press, Cambridge, UK and New York, NY, USA, 488 pp., 2005.

Ivy, D. J., Arnold, T., Harth, C. M., Steele, L. P., Mühle, J., Rigby, M., Salameh, P. K., Leist, M., Krummel, P. B., Fraser, P. J., Weiss, R. F., and Prinn, R. G.: Atmospheric histories and growth trends of C_4F_{10}, C_5F_{12}, C_6F_{14}, C_7F_{16} and C_8F_{18}, Atmos. Chem. Phys., 12, 4313–4325, https://doi.org/10.5194/acp-12-4313-2012, 2012.

Kohno, S. and Shibanuma, T.: Process for the preparation of pentafluoroethane, US Patent 6 175 045, available at: https://www.google.ch/patents/US6175045 (last access: 6 December 2017), 2001.

Langenfelds, R. L., Fraser, P. J., Francey, R. J., Steele, L. P., Porter, L. W., and Allison, C. E.: The Cape Grim air archive: the first seventeen years, 1978–1995, in: Baseline Atmospheric Program (Australia) 1994–95, edited by: Francey, R. J., Dick, A. L., and Derek, N., Australian Bureau of Meteorology and CSIRO Marine and Atmosperic Research, Melbourne, Australia, 53–70, 1996.

Langenfelds, R. L., Krummel, P. B., Fraser, P. J., Steele, L. P., Ward, J., and Somerville, N. T.: Archiving of Cape Grim air, in: Baseline Atmospheric Program Australia 2009–2010, edited by: Derek, N., Krummel, P. B., and Cleland, S. J., 44–45, Australian Bureau of Meteorology and CSIRO Marine and Atmosperic Research, Melbourne, Australia, 2014.

Laube, J. C., Newland, M. J., Hogan, C., Brenninkmeijer, C. A. M., Fraser, P. J., Martinerie, P., Oram, D. E., Reeves, C. E., Röckmann, T., Schwander, J., Witrant, E., and Sturges, W. T.: Newly detected ozone-depleting substances in the atmosphere, Nat. Geosci., 7, 266–269, https://doi.org/10.1038/NGEO2109, 2014.

Laube, J. C., Mohd Hanif, N., Martinerie, P., Gallacher, E., Fraser, P. J., Langenfelds, R., Brenninkmeijer, C. A. M., Schwander, J., Witrant, E., Wang, J.-L., Ou-Yang, C.-F., Gooch, L. J., Reeves, C. E., Sturges, W. T., and Oram, D. E.: Tropospheric observations of CFC-114 and CFC-114a with a focus on long-term trends and emissions, Atmos. Chem. Phys., 16, 15347–15358, https://doi.org/10.5194/acp-16-15347-2016, 2016.

Maione, M., Giostra, U., Arduini, J., Furlani, F., Graziosi, F., Lo Vullo, E., and Bonasoni, P.: Ten years of continuous observations of stratospheric ozone depleting gases at Monte Cimone (Italy) — Comments on the effectiveness of the Montreal Protocol from a regional perspective, Sci. Total Environ., 155–164, https://doi.org/10.1016/j.scitotenv.2012.12.056, 2013.

Martinerie, P., Nourtier-Mazauric, E., Barnola, J.-M., Sturges, W. T., Worton, D. R., Atlas, E., Gohar, L. K., Shine, K. P., and Brasseur, G. P.: Long-lived halocarbon trends and budgets from atmospheric chemistry modelling constrained with measurements in polar firn, Atmos. Chem. Phys., 9, 3911–3934, https://doi.org/10.5194/acp-9-3911-2009, 2009.

Matsunaga, N., Hori, M., and Nagashima, A.: Mutual diffusion coefficients of halogenated-hydrocarbon refrigerant-air systems, in: High Temperatures – High Pressures, 13 ECTP Proceedings, vol. 25, 63–70, 1993.

McCulloch, A. and Lindley, A. A.: From mine to refrigeration: a life cycle inventory analysis of the production of HFC-134a, Int. J. Refrig., 26, 865–872, https://doi.org/10.1016/S0140-7007(03)00095-1, 2003.

Michalak, A. M., Hirsch, A., Bruhwiler, L., Gurney, K. R., Peters, W., and Tans, P. P.: Maximum likelihood estimation of covariance parameters for Bayesian atmospheric trace gas surface flux inversions, J. Geophys. Res.-Atmos., 110, D24107, https://doi.org/10.1029/2005JD005970, 2005.

Miller, B. R., Weiss, R. F., Salameh, P. K., Tanhua, T., Greally, B. R., Mühle, J., and Simmonds, P. G.: Medusa: A sample preconcentration and GC/MS detector system for in situ measurements of atmospheric trace halocarbons, hydro-

carbons, and sulfur compounds, Anal. Chem., 80, 1536–1545, https://doi.org/10.1021/ac702084k, 2008.

Montzka, S. A. and Reimann, S.: Ozone-Depleting Substances (ODSs) and related chemicals, in: Scientific Assessment of Ozone Depletion: 2010, Global Ozone Research and Monitoring Project, Report No. 52, Chapter 1, World Meteorological Organisation, Geneva, Switzerland, 2011.

Myhre, G., Shindell, D., Breon, F.-M., Collins, W., Fuglestvedt, J., Huang, J., Koch, D., Lamarque, J.-F., Lee, D., Mendoza, B., Nakajima, T., Robock, A., Stephens, G., Taekmura, T., and Zhang, H.: Anthropogenic and natural radiative forcing, in: Climate Change 2013: The Physical Science Basis. Contribution of Working Group I to the Fifth Assessment Report of the Intergovernmental Panel on Climate Change, edited by: Stocker, T. F., Qin, D., Plattner, G.-K., Tignor, M., Allen, S. K., Boschung, J., Nauels, A., Xia, Y., Bex, V., and Midgley, P. M., Cambridge University Press, Cambridge, UK and New York, NY, USA, 659–740, 2013.

O'Doherty, S., Simmonds, P. G., Cunnold, D. M., Wang, H. J., Sturrock, G. A., Fraser, P. J., Ryall, D., Derwent, R. G., Weiss, R. F., Salameh, P., Miller, B. R., and Prinn, R. G.: In situ chloroform measurements at Advanced Global Atmospheric Gases Experiment atmosperic research stations from 1994 to 1998, J. Geophys. Res., 106, 20429–20444, https://doi.org/10.1029/2000JD900792, 2001.

O'Doherty, S., Rigby, M., Mühle, J., Ivy, D. J., Miller, B. R., Young, D., Simmonds, P. G., Reimann, S., Vollmer, M. K., Krummel, P. B., Fraser, P. J., Steele, L. P., Dunse, B., Salameh, P. K., Harth, C. M., Arnold, T., Weiss, R. F., Kim, J., Park, S., Li, S., Lunder, C., Hermansen, O., Schmidbauer, N., Zhou, L. X., Yao, B., Wang, R. H. J., Manning, A. J., and Prinn, R. G.: Global emissions of HFC-143a (CH_3CF_3) and HFC-32 (CH_2F_2) from in situ and air archive atmospheric observations, Atmos. Chem. Phys., 14, 9249–9258, https://doi.org/10.5194/acp-14-9249-2014, 2014.

Oram, D. E.: Trends of Long-Lived Anthropogenic Halocarbons in the Southern Hemisphere and Model Calculation of Global Emissions, PhD Thesis, University of East Anglia, UK, 1999.

Penkett, S. A., Prosser, N. J. D., Rasmussen, R. A., and Khalil, M. A. K.: Atmospheric measurements of CF_4 and other fluorocarbons containing the CF_3 grouping, J. Geophys. Res., 86, 5172–5178, https://doi.org/10.1029/JC086iC06p05172, 1981.

Piepho, E., Wilmet, V., and Buyle, O.: Pentafluoroethane production method, US Patent 7 067 707, available at: https://www.google.ch/patents/US7067707 (last access: 6 December 2017), 2006.

Pollock, W. H., Heidt, L. E., Lueb, R. A., Vedder, J. F., Mills, M. J., and Solomon, S.: On the age of stratospheric air and ozone depleption potentials in polar regions, J. Geophys. Res., 97, 12993–12999, https://doi.org/10.1029/92JD01029, 1992.

Prinn, R. G., Weiss, R. F., Fraser, P. J., Simmonds, P. G., Cunnold, D. M., Alyea, F. N., O'Doherty, S., Salameh, P., Miller, B. R., Huang, J., Wang, R. H. J., Hartley, D. E., Harth, C., Steele, L. P., Sturrock, G., Midgley, P. M., and McCulloch, A.: A history of chemically and radiatively important gases in air deduced from ALE/GAGE/AGAGE, J. Geophys. Res., 105, 17751–17792, https://doi.org/10.1029/2000JD900141, 2000.

Rao, V. N. M.: Alternatives to Chlorofluorocarbons (CFCs), in: Organofluorine Chemistry: Principles and Commercial Applications, edited by: Banks, R. E., Smart, B. E., and Tatlow, J. C., Topics in Applied Chemistry, Plenum Press, New York, 159–175, 1994.

Rasmussen, R. A. and Khalil, M. A. K.: Atmospheric halocarbons: measurements and analyses of selected trace gases, Proceedings of the NATO Advanced Study Institute on Atmospheric Ozone, 1002, 209–231, 1980.

Ravishankara, A. R., Solomon, S., Turnipseed, A. A., and Warren, R. F.: Atmospheric lifetimes of long-lived halogenated species, Science, 259, 194–199, 1993.

Rienecker, M. M., Suarez, M. J., Gelaro, R., Todling, R., Bacmeister, J., Liu, E., Bosilovich, M., Schubert, S. D., Takacs, L., Kim, G.-K., Bloom, S., Chen, J., Collins, D., Conaty, A., Da Silva, A., Gu, W., Joiner, J., Koster, R. D., Lucchesi, R., Molod, A., Owens, T., Pawson, S., Pegion, P., Redder, C. R., Reichle, R., Robertson, F. R., Ruddick, A. G., Sienkiewicz, M., and Woollen, J.: MERRA: NASA's modern-era retrospective analysis for research and applications, J. Climate, 24, 3624–3648, https://doi.org/10.1175/JCLI-D-11-00015.1, 2011.

Rigby, M., Ganesan, A. L., and Prinn, R. G.: Deriving emissions from sparse mole-fraction time series, J. Geophys. Res., 116, D08306, https://doi.org/10.1029/2010JD015401, 2011.

Rigby, M., Prinn, R. G., O'Doherty, S., Montzka, S. A., McCulloch, A., Harth, C. M., Mühle, J., Salameh, P. K., Weiss, R. F., Young, D., Simmonds, P. G., Hall, B. D., Dutton, G. S., Nance, D., Mondeel, D. J., Elkins, J. W., Krummel, P. B., Steele, L. P., and Fraser, P. J.: Re-evaluation of the lifetimes of the major CFCs and CH_3CCl_3 using atmospheric trends, Atmos. Chem. Phys., 13, 2691–2702, https://doi.org/10.5194/acp-13-2691-2013, 2013.

Rigby, M., Prinn, R. G., O'Doherty, S., Miller, B. R., Ivy, D., Mühle, J., Harth, C. M., Salameh, P. K., Arnold, T., Weiss, R. F., Krummel, P. B., Steele, L. P., Fraser, P. J., Young, D., and Simmonds, P. G.: Recent and future trends in synthetic greenhouse gas radiative forcing, Geophys. Res. Lett., 41, 2623–2630, https://doi.org/10.1002/2013GL059099, 2014.

Ruckstuhl, A. F., Henne, S., Reimann, S., Steinbacher, M., Vollmer, M. K., O'Doherty, S., Buchmann, B., and Hueglin, C.: Robust extraction of baseline signal of atmospheric trace species using local regression, Atmos. Meas. Tech., 5, 2613–2624, https://doi.org/10.5194/amt-5-2613-2012, 2012.

Sander, S. P., Abbatt, J., Barker, J. R., Burkholder, J. B., Friedl, R. R., Golden, D. M., Huie, R. E., Kolb, C. E., Kurylo, M. J., Moortgart, G. K., Orkin, V. L., and Wine, P. H.: Chemical Kinetics and Photochemical Data for Use in Atmospheric Studies, Evaluation No. 17 of the NASA Panel for Data Evaluation, JPL Publication 10-6, Jet Propulsion Laboratory, Pasadena, 2011.

Schauffler, S. M., Heidt, L. E., Pollock, W. H., Gilpin, T. M., Vedder, J. F., Solomon, S., Lueb, R. A., and Atlas, E. I.: Measurements of halogenated organic compounds near the tropical tropopause, Geophys. Res. Lett., 20, 2567–2570, https://doi.org/10.1029/93GL02840, 1993.

Schoenenberger, F., Vollmer, M. K., Rigby, M., Hill, M., Fraser, P. J., Krummel, P. B., Langenfelds, R. L., Rhee, T. S., Peter, T., and Reimann, S.: First observations, trends and emissions of HCFC-31 (CH_2ClF) in the global atmosphere, Geophys. Res. Lett., 42, 7817–7824, https://doi.org/10.1002/2015GL064709, 2015.

Seibert, P. and Frank, A.: Source-receptor matrix calculation with a Lagrangian particle dispersion model in backward mode, At-

mos. Chem. Phys., 4, 51–63, https://doi.org/10.5194/acp-4-51-2004, 2004.

Shanthan Rao, P., Narsaiah, B., Rambabu, Y., Sridhar, M., and V., R. K.: Catalytic processes for fluorochemicals: sustainable alternatives, in: Industrial Catalysis and Separations: Innovations for Process Intensification, edited by: Raghavan, K. V. and Reddy, B. M., Apple Academic Press, Toronto, 407–435, 2015.

Simmonds, P. G., O'Doherty, S., Nickless, G., Sturrock, G. A., Swaby, R., Knight, P., Ricketts, J., Woffendin, G., and Smith, R.: Automated gas chromatograph mass spectrometer for routine atmospheric field measurements of the CFC replacement compounds, the hydrofluorocarbons and hydrochlorofluorocarbons, Anal. Chem., 67, 717–723, https://doi.org/10.1021/ac00100a005, 1995.

Singh, H. B., Salas, L., Shigeishi, H., and Crawford, A.: Urban-nonurban relationships of halocarbons, SF_6, N_2O, and other atmospheric trace constituents, Atmos. Environ., 11, 819–828, https://doi.org/10.1016/0004-6981(77)90044-0, 1977.

Singh, H. B., Salas, L. J., Shigeishi, H., and Scribner, E.: Atmospheric halocarbons, hydrocarbons, and sulfur hexafluoride: global distribution, sources, and sinks, Science, 203, 899–903, https://doi.org/10.1126/science.203.4383.899, 1979.

Singh, H. B., Salas, L. J., and Stiles, R. E.: Selected man-made halogenated chemicals in the air and oceanic environment, J. Geophys. Res., 88, 3675–3683, https://doi.org/10.1029/JC088iC06p03675, 1983.

SPARC: SPARC Report on the Lifetimes of Stratospheric Ozone-Depleting Substances, Their Replacements, and Related Species, Tech. Rep. 6, WCRP-15/2013, available at: www.sparc-climate.org/publications/sparc-reports/ (last access: 6 December 2017), 2013.

Stemmler, K., Folini, D., Ubl, S., Vollmer, M. K., Reimann, S., O'Doherty, S., Greally, B. R., Simmonds, P. G., and Manning, A. J.: European emissions of HFC-365mfc, a chlorine-free substitute for the foam blowing agents HCFC-141b and CFC-11, Environ. Sci. Technol., 41, 1145–1151, https://doi.org/10.1021/es061298h, 2007.

Stohl, A.: Trajectory statistics – a new method to establish source-receptor relationships of air pollutants and its application to the transport of particulate sulfate in Europe, Atmos. Environ., 30, 579–587, https://doi.org/10.1016/1352-2310(95)00314-2, 1996.

Stohl, A., Forster, C., Frank, A., Seibert, P., and Wotawa, G.: Technical note: The Lagrangian particle dispersion model FLEXPART version 6.2, Atmos. Chem. Phys., 5, 2461–2474, https://doi.org/10.5194/acp-5-2461-2005, 2005.

Sturrock, G. A., Porter, L. W., and Fraser, P. J.: In situ measurement of CFC replacement chemicals and other halocarbons at Cape Grim: the AGAGE GC-MS Program, Baseline atmospheric program (Australia), 1997–1998, 43–49, 2001.

Sturrock, G. A., Etheridge, D. M., Trudinger, C. M., Fraser, P. J., and Smith, A. M.: Atmospheric histories of halocarbons from analysis of Antarctic firn air: Major Montreal Protocol species, J. Geophys. Res., 107, 4765, https://doi.org/10.1029/2002JD002548, 2002.

Toms, G. S., Frank, M. V., and Bein, T. W.: Navy shipboard CFC-114 elimination program, Nav. Eng. J., 116, 55–68, 2004.

Totterdill, A., Kovács, T., Feng, W., Dhomse, S., Smith, C. J., Gómez-Martín, J. C., Chipperfield, M. P., Forster, P. M., and Plane, J. M. C.: Atmospheric lifetimes, infrared absorption spectra, radiative forcings and global warming potentials of NF_3 and CF_3CF_2Cl (CFC-115), Atmos. Chem. Phys., 16, 11451–11463, https://doi.org/10.5194/acp-16-11451-2016, 2016

Trudinger, C. M., Enting, I. G., Etheridge, D. M., Francey, R. J., Levchenko, V. A., Steele, L. P., Raynaud, D., and Arnaud, L.: Modeling air movement and bubble trapping in firn, J. Geophys. Res., 102, 6747–6763, https://doi.org/10.1029/96JD03382, 1997.

Trudinger, C. M., Etheridge, D. M., Rayner, P. J., Enting, I. G., Sturrock, G. A., and Langenfelds, R. L.: Reconstructing atmospheric histories from measurements of air composition in firn, J. Geophys. Res., 107, 4780, https://doi.org/10.1029/2002JD002545, 2002.

Trudinger, C. M., Enting, I. G., Rayner, P. J., Etheridge, D. M., Buizert, C., Rubino, M., Krummel, P. B., and Blunier, T.: How well do different tracers constrain the firn diffusivity profile?, Atmos. Chem. Phys., 13, 1485–1510, https://doi.org/10.5194/acp-13-1485-2013, 2013.

Trudinger, C. M., Fraser, P. J., Etheridge, D. M., Sturges, W. T., Vollmer, M. K., Rigby, M., Martinerie, P., Mühle, J., Worton, D. R., Krummel, P. B., Steele, L. P., Miller, B. R., Laube, J., Mani, F. S., Rayner, P. J., Harth, C. M., Witrant, E., Blunier, T., Schwander, J., O'Doherty, S., and Battle, M.: Atmospheric abundance and global emissions of perfluorocarbons CF_4, C_2F_6 and C_3F_8 since 1800 inferred from ice core, firn, air archive and in situ measurements, Atmos. Chem. Phys., 16, 11733–11754, https://doi.org/10.5194/acp-16-11733-2016, 2016.

UNEP: Handbook for the Montreal Protocol on Substances that Deplete the Ozone Layer, 11th edn., United Nations Environment Programme, Ozone Secretariat, Nairobi, Kenya, available at: http://www.ozone.unep.org, 781 pp., last access: 6 December 2017.

UNEP/TEAP: Assessment of alternatives to HCFCs and HFCs and update of the TEAP 2005 supplement report data, in: Task Force Decision XX/8 Report, vol. 1, United Nations Environment Programme, Ozone Secretariat, Nairobi, Kenya, available at: http://www.ozone.unep.org (last access: 6 December 2017), 129 pp., 2009.

Velders, G. J. M. and Daniel, J. S.: Uncertainty analysis of projections of ozone-depleting substances: mixing ratios, EESC, ODPs, and GWPs, Atmos. Chem. Phys., 14, 2757–2776, https://doi.org/10.5194/acp-14-2757-2014, 2014.

Vollmer, M. K., Miller, B. R., Rigby, M., Reimann, S., Mühle, J., Krummel, P. B., O'Doherty, S., J., K., Rhee, T. S., Weiss, R. F., Fraser, P. J., Simmonds, P. G., Salameh, P. K., Harth, C. M., Wang, R. H. J., Steele, L. P., Young, D., Lunder, C. R., Hermansen, O., Ivy, D., Arnold, T., Schmidbauer, N., Kim, K.-R., Greally, B. R., Hill, M., Leist, M., Wenger, A., and Prinn, R. G.: Atmospheric histories and global emissions of the anthropogenic hydrofluorocarbons HFC-365mfc, HFC-245fa, HFC-227ea, and HFC-236fa, J. Geophys. Res., 116, D08304, https://doi.org/10.1029/2010JD015309, 2011.

Vollmer, M. K., Reimann, S., Hill, M., and Brunner, D.: First observations of the fourth generation synthetic halocarbons HFC-1234yf, HFC-1234ze(E), and HCFC-1233zd(E) in the atmosphere, Environ. Sci. Technol., 49, 2703–2708, https://doi.org/10.1021/es505123x, 2015a.

Vollmer, M. K., Rhee, T. S., Rigby, M., Hofstetter, D., Hill, M., Schoenenberger, F., and Reimann, S.: Modern inhalation anesthetics: Potent greenhouse gases in the global atmosphere, Geophys. Res. Lett., 42, 1606–1611, https://doi.org/10.1002/2014GL062785, 2015b.

Vollmer, M. K., Rigby, M., Laube, J. C., Henne, S., Rhee, T. S., Gooch, L. J., Wenger, A., Young, D., Steele, L. P., Langenfelds, R. L., Brenninkmeijer, C. A. M., Wang, J.-L., Ou-Yang, C.-F., Wyss, S. A., Hill, M., Oram, D. E., Krummel, P. B., Schoenenberger, F., Zellweger, C., Fraser, P. J., Sturges, W. T., O'Doherty, S., and Reimann, S.: Abrupt reversal in emissions and atmospheric abundance of HCFC-133a (CF_3CH_2Cl), Geophys. Res. Lett., 42, 8702–8710, https://doi.org/10.1002/2015GL065846, 2015c.

Vollmer, M. K., Mühle, J., Trudinger, C. M., Rigby, M., Montzka, S. A., Harth, C. M., Miller, B. R., Henne, S., Krummel, P. B., Hall, B. D., Young, D., Kim, J., Arduini, J., Wenger, A., Yao, B., Reimann, S., O'Doherty, S., Maione, M., Etheridge, D. M., Li, S., Verdonik, D. P., Park, S., Dutton, G., Steele, L. P., Lunder, C. R., Rhee, T. S., Hermansen, O., Schmidbauer, N., Wang, R. H. J., Hill, M., Salameh, P. K., Langenfelds, R. L., Zhou, L., Blunier, T., Schwander, J., Elkins, J. W., Butler, J. H., Simmonds, P. G., Weiss, R. F., Prinn, R. G., and Fraser, P. J.: Atmospheric histories and global emissions of halons H-1211 ($CBrClF_2$), H-1301 ($CBrF_3$), and H-2402 ($CBrF_2CBrF_2$), J. Geophys. Res.-Atmos., 121, 3663–3686, https://doi.org/10.1002/2015JD024488, 2016.